**US Army Corps
of Engineers**
Waterways Experiment
Station

Microwave Dielectric Behavior of Soils

Report 2
A Unique Coaxial Measurement Apparatus

*by   John O. Curtis
Environmental Laboratory*

DTIC
SELECTE
FEB 2 4 1994
S
B
D

94-05753

94 2 23   002

The contents of this report are not to be used for advertising, publication, or promotional purposes. Citation of trade names does not constitute an official endorsement or approval of the use of such commercial products.

Microwave Dielectric Behavior of Soils

Report 2
A Unique Coaxial Measurement Apparatus

by   John O. Curtis
     Environmental Laboratory

     U.S. Army Corps of Engineers
     Waterways Experiment Station
     3909 Halls Ferry Road
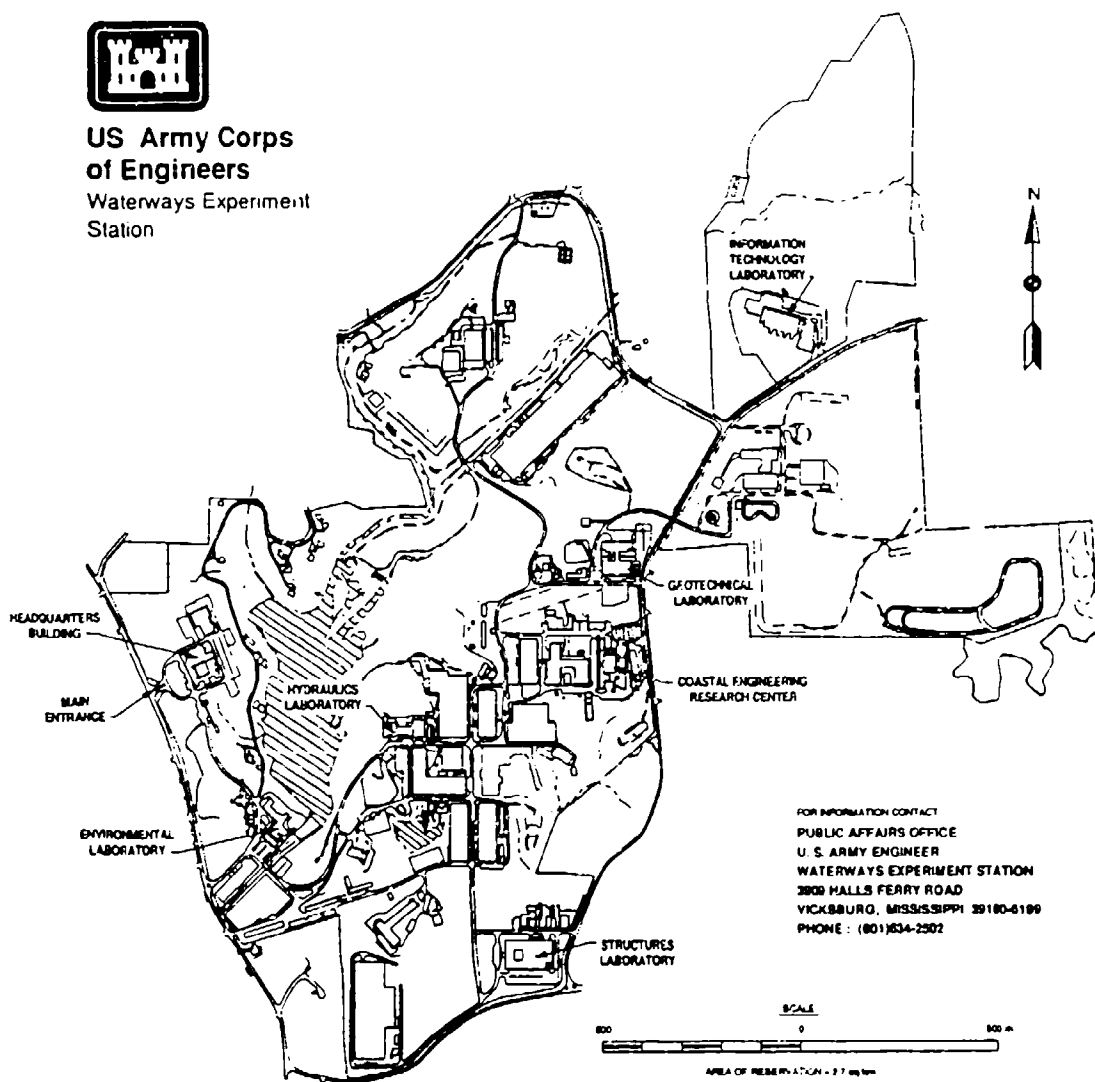   Vicksburg, MS   39180-6199

Report 2 of a series

US Army Corps
of Engineers
Waterways Experiment
Station

Contents

List of Figures

iii

Preface

The study reported herein was conducted within the facilities of the Environmental Laboratory (EL) of the U.S. Army Engineer Waterways Experiment Station (WES) during the period of May 1991 to June 1992 for Headquarters, U.S. Army Corps of Engineers.

General supervision was provided by Drs. Daniel Cress and Victor Barber, Acting Chiefs, Environmental Systems Division (ESD), EL, Dr. Raymond L. Montgomery, Chief, Environmental Engineering Division, EL, and Dr. John Harrison, Director, EL.

Dr. John O. Curtis developed the experimental procedure reported herein and prepared the report under the direct supervision of Messrs. Malcolm Keown and Kenneth Hall, Chiefs, Environmental Constraints Group, ESD.

At the time of publication of this report, Director of WES was Dr. Robert W. Whalin. Commander was COL Bruce K. Howard, EN.

This report should be cited as follows:

v

1   Introduction

New and improved methods of remote sensing have increased the understanding of Earth's origins, its resources, and those processes that contribute to its dynamic (on a large time scale) nature. Scientists and engineers from many disciplines are constantly exploring new ways to quantify the Earth's properties for their particular applications. Among these methods are measurements of electromagnetic energy in many different wavelength regimes, both passive and active. The development of small powerful sources and ultrasensitive receivers along with improved data processing capabilities has fostered renewed interest in measurements of the Earth within the microwave region of the spectrum where wavelengths in air range from a few millimeters to several meters.

Natural terrain surfaces consist of bare soils, rocks, vegetation, and water. This study was initiated with the hope of making a meaningful contribution to the understanding of microwave interactions with natural terrain. The first report in this series attempts to summarize what is currently known about the measurement and modeling of the electrical properties of well-characterized soils (Curtis, In Preparation). This report contains a description of a new dielectric property measurement capability recently developed at the U.S. Army Engineer Waterways Experiment Station in Vicksburg, MS, that will be used in the future to establish a comprehensive database of soil properties covering a broad spectrum of soil types, measurement frequencies, sample moisture contents, and sample temperatures. The final report of the series will present some initial measurement results and will discuss two modeling approaches to interpreting those data. Most of the information contained in this series of reports is drawn from a doctoral research program recently completed by the author (Curtis 1992).

In an effort to make each report of this series as self-contained as possible, the rationale for pursuing this research program as well as some supporting information in appendices is included within each document. It is hoped that this will be useful for the individual who might read only one of the reports.

Reasons for Studying Electrical Properties of Soils

Soil moisture measurements

The dominant factor that controls the electrical behaviou of soils is the presence of water (Topp, Davis, and Annan 1980). Obviously, one would hope to take advantage of this experimental fact to develop a means of accurately and quickly measuring the moisture in soils without having to collect numerous samples in the field, weigh them, dry them for extended periods of time, and weigh them again to obtain either a gravimetric (weight of water/weight of dry soil) moisture content or a more useful volumetric (volume of water/volume of soil sample) moisture content.

Numerous attempts have been made to develop a useful method for measuring soil moisture content. All have met with varying degrees of success, and none has proven accurate under all conditions. For example, a technique that essentially amounts to burying radar transmit and receive antennas in the soil and relating the measurements of attenuated received signals to moisture content (Birchak et al. 1974) is destructive to the soil fabric (the way in which soil particles are arranged), is very much controlled by the fabric and the size distribution of particles, and precludes the use of the same instrument in multiple locations (nature is not homogeneous) as well as the ability to easily repair defective equipment.

Another approach taken by some researchers for making field measurements of soil moisture (that also has numerous application in the biomedical field) is that of measuring the change in fringe capacitance of an open-ended coaxial probe (Thomas 1966; Brunfeldt 1987; Gabriel, Grant, and Young 1986). When pressed against a soil whose properties are unknown, the resulting change in capacitance produced by the impedance mismatch is related to electrical properties through calibration relationships. Problems arising from these measurements include the need to have proper contact between the probe tip and the soil surface, the fact that the volume of material associated with the fringe capacitance is quite small (1 cm^3 or less), and that calibration conditions simply cannot account for all of the dielectric loss mechanisms that exist in natural soils. The losses in moist soils can be highly frequency dependent over a range of several frequency decades on the electromagnetic spectrum. A recent variation on the open-ended probe measurement scheme involves the use of a waveguide section instead of a coaxial device (Parchomchuk, Wallender, and King 1990).

The concern over small sample volumes can be overcome with a redesign of the open-ended coaxial probe that replaces the solid outer conductor with several pointed tines (Campbell 1988) which allows for the probe to be pushed into the surface of soft soils. The volume of soil enclosed by such probes can easily be tens of cubic centimeters. The tined coaxial probes that have been built to date operate in a frequency range that is very much subject to the material-dependent loss mechanisms alluded to above. Research continues that

2

is directed to better understanding these various mechanisms and to fabricate a probe that operates in a frequency range that is not subject to such material-dependent anomalies.

Subterranean investigations

There are many types of electrical measurements in soils (and rocks) that are used to understand what lies beneath the Earth's surface (Telford et al. 1984). Among these are various schemes for measuring soil resistivity as well as the attenuation of propagating electromagnetic waves.

Resistivity measurements. Resistivity data in soils are collected by injecting known currents (usually of a frequency less than 60 Hz; alternating current required to minimize effects of charge buildup on the probe) into the ground and measuring potential differences across pairs of nearby electrodes. Assuming homogeneous media and uniform resistivity, it is possible to calculate from the potential differences an apparent resistivity of the earth material. These measurements will be affected by the presence of water in the soil or rock, by the presence of mineral compounds that could go into ionic solution with available water, and by the physical structure of the subsurface terrain itself. This being the case, resistivity measurements are useful as a measure of subsurface water volume, the locations of mineral deposits, and subsurface structure.

Electromagnetic wave propagation. Another method of making electrical subsurface measurements involves the transmission of electromagnetic waves into the soil and detection of energy that results from waves reflected from subsurface anomalies. Having the ability to track wave propagation in time, either by pulsing the source or sweeping over a known frequency band in some controlled manner, means that electromagnetic wave propagation methods of subterranean investigations are particularly useful for locating the depth of electrical anomalies such as the water table in sandy soil (Olhoeft 1983; Stewart 1982; Wright, Olhoeft, and Watts 1984), buried pipes or wires, or cavities such as tunnels or caves (Ballard 1983). Other applications include the delineation of stratified media (Lundien 1972) and determination of the thickness of ice and frost layers (Jakkula, Ylinen, and Tiuri 19c_, O'Neill and Arcone 1991).

There are some practical bounds on the utility of radio frequency systems to conduct subterranean investigations because of the phenomenon of "skin depth," a measure of the attenuation of the electromagnetic energy as it travels through the medium. For relatively low-frequency sources (approximately 200 MHz), it can be shown that low-loss soils such as dry sands can possess a skin depth of approximately 10 to 15 m, while high-loss soils such as wet silts and clays may have skin depths of only a few centimeters. Modern radio frequency receivers are extremely sensitive devices, often having a dynamic range of 50 to 100 db. The signal at skin depth represents about an 8.7-db loss in power or a two-way loss at the receiver for reflected signals of about

17.4 db. It is certainly not inconceivable that radio frequency receivers should be capable of successfully detecting reflected signals from subterranean anomalies at depths of two to three skin depths or more.

Remote sensing of environment

Virtually all remote sensing of the environment from airborne or spaceborne platforms involves the measurement of electromagnetic radiation from the Earth's surface and/or atmosphere. Passive surveillance involves measurements of emitted radiation and that reflected from natural sources such as the sun, the atmosphere, and surrounding terrain. Active remote sensing measurement systems include a source for illuminating the target of interest. Whether passive or active, visual, thermal infrared, microwave, or millimeter wave sensors are utilized, remote sensing is the collection and interpretation of electromagnetic radiation and, as such, demands an understanding of the dielectric properties of those materials being observed.

Environmental remote sensing applications form a list that grows yearly as electronic components are improved and data collection and processing hardware and software become faster, more reliable, and less costly. For example, satellites can provide worldwide surveys of land-use patterns to monitor the threat of urbanization, waste disposal, and erosion of the land (Colwell 1983). Similar systems (including those mounted in aircraft) can monitor the health of vegetation to keep abreast of such things as loss of forest and the potential for food shortages. Sea traffic in the far northern and southern shipping lanes can be made safer through the use of airborne and spaceborne sensors to detect ice hazards.

One of the more obvious applications for microwave remote sensing devices is that of conducting surface moisture surveys to help predict ground-water availability and the potential for flooding. Attempts have been made to relate soil moisture to both laboratory reflectance data (Lundien 1966) and to airborne sensor backscatter measurements (Ulaby, Cihlar, and Moore 1974; John 1992). Careful airborne sensor measurements might provide a first approximation to the complex dielectric constant of the soil near the surface.

Because of the difference in dielectric behavior of liquid water and various forms of ice, it may be possible to use airborne sensors to detect freezing and thawing (Wegmuller 1990) in remote locations that could be used to predict spring runoff conditions and all that that encompasses for agricultural applications, the effects on the fishing industry, and the anticipation of flooding in built-up areas. Military analysts are concerned about soil moisture conditions because of its impact on trafficability, the ability of vehicles to move effectively over natural terrain.

Another remote sensing application is the mapping of exposed soils and rocks in remote areas of the world from high-flying aircraft or satellites, which might prove useful for geomorphological studies (Swanson et al. 1988)

4

or even mineral exploration. A less obvious, but recent, application of micro-wave remote sensing in soils dealt with archeological surveys in desert areas (Berlin et al. 1986; McCauley et al. 1986).

Others

While the above paragraphs emphasize some of the most obvious and useful applications of a better understanding of soil electrical properties, others have been noted in the literature. For example, some researchers have attempted to relate electrical property measurements to the physical properties of soils (Campbell and Ulrichs 1969; Hayre 1970; Arulanandan and Smith 1973; Madden 1974). Of course, nothing has been said about the military's need to better understand the microwave response of soils that form the backgrounds to military targets; i.e., when and why does clutter become a source of target-like signatures? Outside of the topic of soils, studies of the microwave response of foodstuffs has direct application to quality control concerns in the food industry (Nelson 1973; Nelson 1983).

Another new application of this technology that is closely related to the discussion on soil moisture is that of detecting liquid ground contaminants, either near the surface or at arbitrary depths using a specially fabricated probe. If, as will be argued later, polarizable liquids can be characterized by a unique frequency of peak losses because of the dielectric relaxation phenomenon, then a probe could be designed to measure losses over a frequency span that is broad enough to detect a peak loss frequency and, coupled with the results of a thorough experimental program, to identify the particular contaminant.

Problem Statement

The overall objective of this research is to measure and model the dielectric response of moist soils in ways that will test the current understanding of loss mechanisms over a broad range of moisture levels, frequencies, and material temperatures and perhaps suggest new ways of thinking about losses as a function of these variables.

What is first required to help achieve this objective is an apparatus that will allow for the measurement of attenuation in moist soils over a broad spectrum of frequencies while maintaining a required sample temperature. A methodology must exist for allowing sample moisture to vary in a measurable way. The remainder of this report describes such a device and a methodology and includes measured data that substantiates the algorithm used to compute values of the complex dielectric constant for each set of variables.

2 A Coaxial Apparatus for Dielectric Measurements

The choices for laboratory techniques for making material electrical property measurements include resonant cavity, waveguide, and coaxial, with some new work being done on hybrids of the latter two (Taherian et al. 1991). Resonant cavity applications are limited to small volumes of material, which could present a problem with trying to measure the homogeneous response of substances like sands, which are highly nonhomogeneous at small scales. Waveguide measurements are very sensitive to how the sections are mated (and how repeatable are those connections). While they involve adequate volumes of material, sample preparation is not likely to produce a uniform density for granular materials, as the substance must be poured into one end and tamped to fill the volume. Dielectric seals would be required to provide a plane interface and must be accounted for properly. The literature also indicates that any phase shifts because of nonideal calibrations are nonlinear functions of frequency and must be accounted for during processing of the data. Waveguards also possess a cutoff frequency below which plane waves cannot propagate. As is true for waveguides, the usual coaxial devices (beadless air lines) suffer from the problems of uniform sample preparation and, in fact, are best suited to measuring solid cylinders of material that must be precisely machined to provide a snug fit within the measurement cavity. However, coaxial lines allow plane waves to propagate at all frequencies. Given all of these considerations, a unique coaxial sample holder was designed and fabricated for use in these experiments to provide a practical tradeoff among sample volume, repeatability of connections, and the ability to prepare uniform samples.

Measurement System

A schematic of the measurement system used to conduct these experiments is shown in Figure 1. The electronic equipment that was available is not that which would normally be used for making material electrical property measurements, but it was successfully adapted for this use.
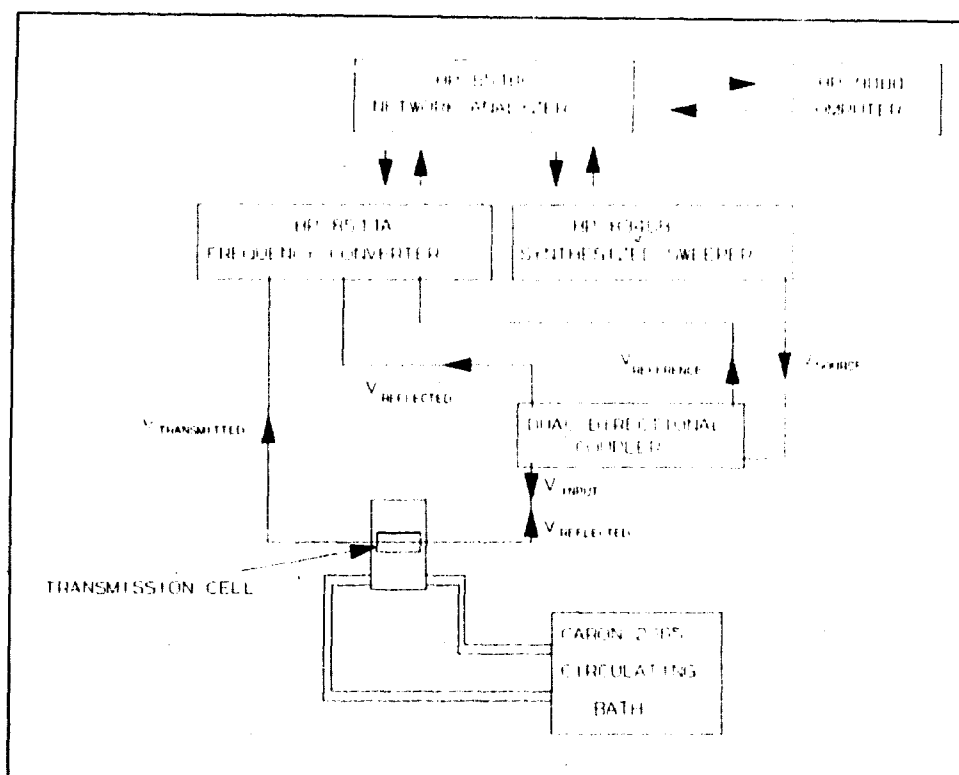
Figure 1. Experimental measurement system

The Hewlett-Packard 8510C Vector Network Analyzer (Hewlett-Packard 1991) is a laboratory device designed to measure the magnitude and phase characteristics of electronic networks and/or components. It consists of a detector unit that measures analog signals in up to four different channels, down converts the signals to an intermediate frequency of 100 kHz, performs an analog-to-digital conversion, and sends those data to a data processing unit that provides a display of the desired quantities. The HP 8510C directs the signal source (in this case, an HP 8340B Synthesized Sweeper) to generate a sinusoidal signal at a specific frequency and directs a test set (an HP 8511A Frequency Converter) to act as the receiver for up to four channels of information that undergo a first frequency conversion to about 20 MHz through the process of harmonic mixing before being sent to the detector unit described above.

The combined dual-directional coupler and frequency converter serves as a substitute for a special test set called the S-Parameter Test Set, which is usually used for such measurements (Hewlett-Packard 1985). The S-Parameter Test Set contains power splitters, coupling devices, and means of establishing equal circuit electrical lengths where appropriate that are transparent to the user. An S-Parameter Test Set would make measurements of signals sent through the transmission cell in both directions. As long as one believes that the material response is not dependent on which direction current flows through the sample, then the reverse measurements should be redundant.

Figure 2 is a photograph of one of the two nearly identical sample holders that were fabricated for these measurements. It was made from 4.5-mm brass stock and provides a square cross-sectional coaxial test volume that is 7.5 mm² and 40 mm long. A piece of copper bus wire was soldered into place as the center conductor, connecting the two 50-ohm SMA-type connectors at each end of the sample holder. The value of sample volume for each holder was estimated, by length measurements, to be 2.21 cm³.
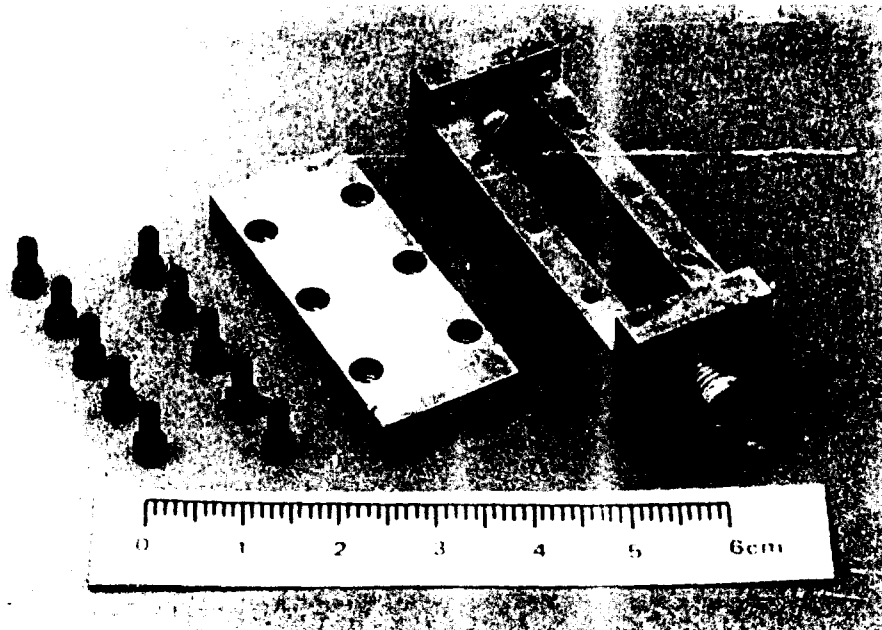
Figure 2.   One of the brass, coaxial sample holders

One area of concern with this sample holder deals with the development of higher order transverse modes. Theory says that a coaxial device should support only the transverse electromagnetic mode as long as the wavelength in the material is greater than twice the cavity width (Stratton 1941). Thus, if the cavity is empty, the highest frequency allowed for these measurements would be

$$(f_{max})_{air} = \frac{v}{\lambda} = \frac{c}{n\lambda} = \frac{3 \times 10^{10} \ cm/sec}{\sqrt{1} \times 1.5 \ cm/cycle} = 20 \ GHz \tag{1}$$

where

v = wave velocity in the material

λ = wavelength

n = index of refraction for the material in the cavity

8

c = speed of light in a vacuum

while for pure water

$$\left(f_{max}\right)_{water} \approx \frac{3 \times 10^{10}}{\sqrt{80} \; x \; 1.5} = 2.24 \; GHz \tag{2}$$

Plane wave conditions for measurements of moist soils should, therefore, exist at some intermediate frequency.

A Caron Model 2065 Circulating Bath was used to provide sample temperature control. The bath was connected to a hollowed aluminum heat source/sink with insulated plastic tubing. As the circulating 50/50 antifreeze solution controlled the physical temperature of the source/sink, it also controlled the temperature of the brass sample holder, which was positioned in a slot in the top of the source/sink and covered with an insulating styrofoam cap.

Governing Equation

Consider the geometry of the coaxial measurement device and the voltages V_i in all regions as shown schematically in Figure 3. A relatively simple governing equation that relates the sample properties and dimension to quantities that can be measured by the network analyzer system can be developed by proper consideration of the boundary conditions.
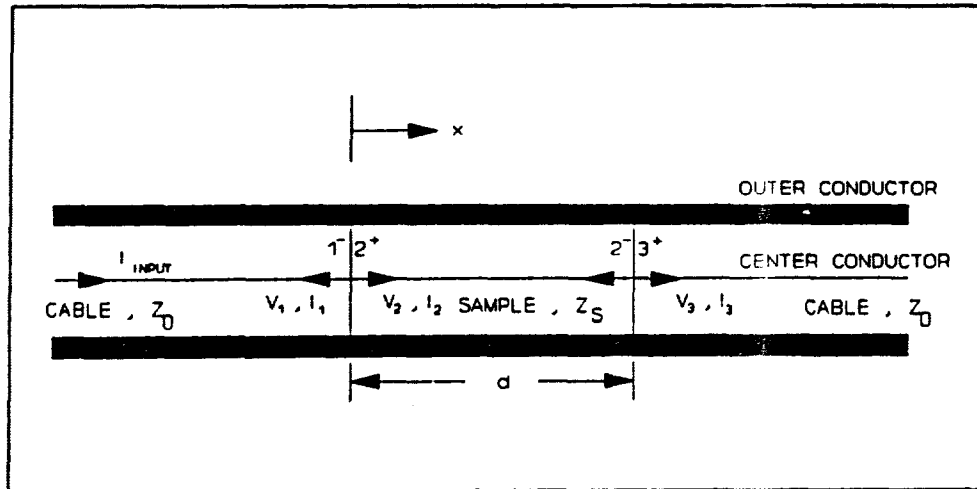
Figure 3.   Sample geometry and voltage and current notation

Using the customary notation for spatial variation of transverse voltages V_i within the cables and sample and considering a snapshot in time (without loss of generality, let time be zero), one can write

$$V_1 = V_{inp}e^{+ik_ox} + V_1^-e^{-ik_ox} \qquad\qquad x < 0$$

$$V_2 = V_2^+ e^{+ik_sx} + V_2^- e^{-ik_sx} \qquad\qquad 0 < x < d \qquad\qquad (3)$$

$$V_3 = V_3^+ e^{+ik_o(x-d)} \qquad\qquad x > d$$

where the k's are the complex propagation constants and contain all of the material electrical property information (see Appendix A). Similar expressions for the center conductor current can be written by taking advantage of the definition of the characteristic impedance of the coaxial line as being the ratio of transverse voltage to the conduction current along the center conductor (Stratton 1941).

$$I_1 = \frac{1}{Z_o}\left(+V_{inp}e^{+ik_ox} - V_1^-e^{-ik_ox}\right) \qquad x < 0$$

$$I_2 = \frac{1}{Z_s}\left(+V_2^+e^{+ik_sx} - V_2^-e^{-ik_sx}\right) \qquad 0 < x < d \qquad\qquad (4)$$

$$I_3 = \frac{1}{Z_o}\left(+V_3^+e^{+ik_o(x-d)}\right) \qquad\qquad x > d$$

where the Z's are the characteristic impedances within each section of the line.

The boundary conditions that can be applied to the geometry shown in Figure 6 are that the tangential field components at the interfaces are continuous and, from the steady-state continuity relationship, that the currents are also continuous across the interfaces. In equation form, these boundary conditions reduce to

$$V_1 = V_2 \ @ \ x = 0 \ : \ V_{inp} + V_1^- = V_2^{+} + V_2^- \qquad (5)$$

$$V_2 = V_3 \ @ \ x = d \ : \ V_2^{+} e^{+ik_s d} + V_2^- e^{-ik_s d} = V_3^{+} \qquad (6)$$

$$I_1 = I_2 \ @ \ x = 0 \ : \ \frac{+V_{inp} - V_1^-}{Z_0} = \frac{+V_2^{+} - V_2^-}{Z_s} \qquad (7)$$

$$I_2 = I_3 \ @ \ x = d \ : \ \frac{+V_2^{+} e^{+ik_s d} - V_2^- e^{-ik_s d}}{Z_s} = \frac{+V_3^{+}}{Z_0} \qquad (8)$$

Not being able to measure V^+_2 or V^-_2 but certainly being able to obtain a reading on the other voltages, the two voltage amplitudes inside the material can be eliminated by adding together Equations 5 and 7 and by taking their difference:

$$V_2^{+} = \frac{1}{2} \left[V_{inp} + V_1^- + \frac{Z_s}{Z_0}\left(V_{inp} - V_1^-\right) \right] \qquad (9)$$

$$V_2^- = \frac{1}{2} \left[V_{inp} + V_1^- - \frac{Z_s}{Z_0}\left(V_{inp} - V_1^-\right) \right] \qquad (10)$$

Substituting these results into Equation 6, one has

$$V_3^{+} = \frac{1}{2} \left[V_{inp} + V_1^- + \frac{Z_s}{Z_0} (V_{inp} - V_1^-) \right] e^{+ik_s d}$$

$$\qquad (11)$$

$$+ \frac{1}{2} \left[V_{inp} + V_1^- - \frac{Z_s}{Z_0} \left(V_{inp} - V_1^-\right) \right] e^{-ik_s d}$$

Normalizing to V_{inp} and collecting terms,

$$\left[1+\frac{V_1^-}{V_{inp}}\right]\cos(k_s d) + i\left[1-\frac{V_1^-}{V_{inp}}\right]\frac{Z_s}{Z_0}\sin(k_s d) = \frac{V_3^*}{V_{inp}} \quad (12)$$

A similar relationship can be written from Equation 8

$$\left[1-\frac{V_1^-}{V_{inp}}\right]\frac{Z_s}{Z_0}\cos(k_s d) + i\left[1+\frac{V_1^-}{V_{inp}}\right]\sin(k_s d) = \frac{Z_s}{Z_0}\frac{V_3^*}{V_{inp}}. \quad (13)$$

It is further convenient to eliminate the characteristic impedances by solving each of the last two equations for Z_s/Z_0 and setting the two expressions equal:

$$\frac{\dfrac{V_3^*}{V_{inp}}-\left[1+\dfrac{V_1^-}{V_{inp}}\right]\cos(k_s d)}{+i\left[1-\dfrac{V_1^-}{V_{inp}}\right]\sin(k_s d)}=\frac{+i\left[1+\dfrac{V_1^-}{V_{inp}}\right]\sin(k_s d)}{\dfrac{V_3^*}{V_{inp}}-\left[1-\dfrac{V_1^-}{V_{inp}}\right]\cos(k_s d)} \quad (14)$$

Simplifying,

$$\cos(k_s d)=\frac{1+\left[\dfrac{V_3^*}{V_{inp}}\right]^2-\left[\dfrac{V_1^-}{V_{inp}}\right]^2}{2\left[\dfrac{V_3^*}{V_{inp}}\right]} \quad (15)$$

Now, following an appropriate calibration of the measurement apparatus, the network analyzer effectively measures V_1^-/V_{inp} and V_3^*/V_{inp}. They are designated, using standard "S", or scattering parameter notation, as S_{11} and S_{21}, respectively. The definition of these "S" parameters requires that there be no current traveling into the sample from the right side of Figure 3. This implies that all circuitry and connectors on the transmission side of the sample are perfectly matched so that no energy is reflected back to the sample. Although this is an assumption for this derivation, the fact that proper equipment was not available for these measurements and that a less than desirable

12

calibration technique was used (described in the next section) makes this idealized configuration quite unlikely.

Using the relationships between the propagation constant and material properties (Appendix A) and assuming nonmagnetic materials, one can then write down the final form of the governing equation:

$$\cos\left[\omega d \frac{\sqrt{\varepsilon}}{c}\right] = \frac{1 + (S_{21})^2 - (S_{11})^2}{2S_{21}} = W_c' \tag{16}$$

This form of the governing equation was reported by Campbell (1990). An earlier derivation, although arriving at a different solution technique, has also been recently discovered (Hewlett-Packard 1985).

The process for calculating values of the complex dielectric constant can now be outlined:

   a. At a given frequency, measure the complex values of S_{11} and S_{21}.

   b. Compute $\cos^{-1}(W_c') = \omega d \frac{\sqrt{\varepsilon}}{c}$.

   c. Square both sides of this expression and solve for ε.

The procedure is not as straightforward as it seems because of a problem with principal values of the $\cos^{-1}$ function. One method for solving for the $\cos^{-1}$ function yields the following (Zucker 1972):

$$\cos^{-1}(W_c') = -i \ln(re^{i\theta}) = \theta - i \ln(r) \tag{17}$$

where

$$re^{i\theta} = W_c' + \sqrt{(W_c')^2 - 1}$$

A great deal of time was spent developing a calculation procedure for Equation 17 that would yield the correct values of ε' and ε''. However, it was later discovered that the calculation routine for the inverse complex cosine function that resides in the HP BASIC compiler within the HP9000 system controller gave exactly the same results. The only difficulty is that, depending on where W_c lies in complex space, the $\cos^{-1}(W_c)$ value computed using the available routines returns real and imaginary components that are both

negative, or having opposite signs. A set of rules had to be developed to
select the sensible results; namely, those that would yield positive values of ϵ'
and ϵ''.

The real part of $\omega d\sqrt{\epsilon}/c$ is a measure of the number of wavelengths
(expressed in radians) of signal that can be contained within the sample holder
at the given radial frequency. The value of θ that is returned by the above
solution algorithm is a principal value, being bounded by $\pm\pi$. However, any
multiple of 2π can be added to θ and give the same result. It turns out that
there is a sensible way of determining how many multiples of 2π to add. One
can either estimate the properties of the material to establish the correct value
of Θ, or one can use the value of "group delay," which is calculated by the
network analyzer to establish the correct value of θ. Group delay is defined
as the signal transit time through a test device (Hewlett-Packard 1991). What
the designers of the network analyzer assumed is that the phase for the wave
in the material is a term like "ωt". Therefore, group delay, or the derivative
of phase with respect to radial frequency is a number with dimensions of time
and interpreted as the time required to transit the sample. An estimate of the
initial value of the number of cycles (multiples of 2π) to add to θ was taken as
the truncated product of group delay and frequency.

Appendix B contains a listing of the HP BASIC code that was developed
by the author to control the data collection system, create a permanent data
file of amplitude and phase measurements as a function of frequency, and
produce a real-time plot of computed complex dielectric constant values.

Experimental Procedure

Calibration

Because of the arrangement and type of measurement apparatus used for
these studies, the most appropriate calibration was found to be the One-Path,
2-Port calibration combined with the adapter-switching technique (Hewlett-
Packard 1991). During this procedure, reflection and transmission cables
were first connected with a thru adapter from an HP85052B, 3.5mm
Calibration Kit, and forward transmission and forward match measurements
were conducted. Next, an equivalent adapter (male-female) from the same Kit
was connected to the input (reflection) cable, and three reflection standards
were measured. These standards were an offset short, an offset open, and a
broadband load, all from the same Calibration Kit. The net result of the
calibration procedure is that the S_{11} measurement effectively takes place at the
bead interface in the SMA connector on the reflection side of the sample
holder, and the S_{21} measurement effectively takes place at the bead interface
in the connector on the transmission side of the holder.

Because of the physical separation of the calibration planes and the inter-
face between the sample and the connector on the end of the holder, an

Because of the physical separation of the calibration planes and the interface between the sample and the connector on the end of the holder, an additional phase shift needed to be added to the S_{11} parameter and subtracted from the S_{21} parameter to make the measured quantities consistent with what was defined in the earlier derivation of the governing equation. Referring to the sketch in Figure 4, the reflected signal must travel an additional distance of 2a beyond the calibration plane to be recorded in the frequency converter. The transmitted signal travels an additional distance of a+b. For these measurements, a = b, and the required phase shift was found to be about 80 picoseconds from measurements of the empty holder.
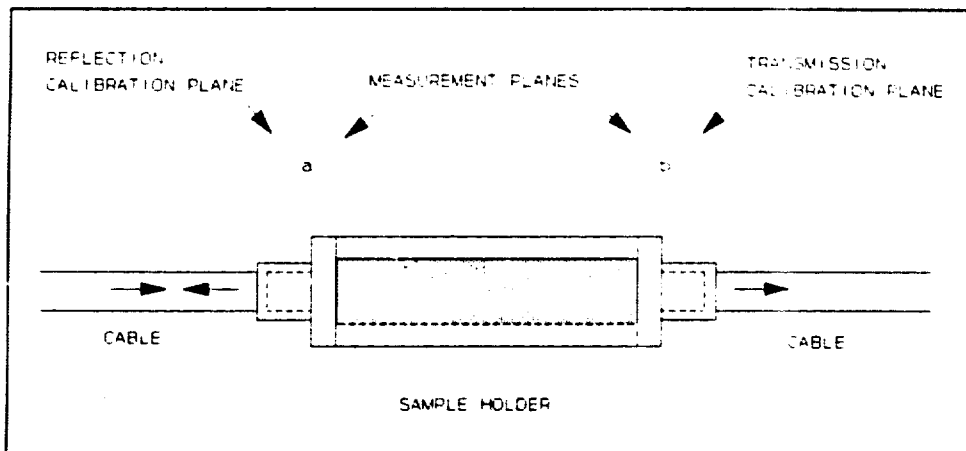
Figure 4. Calibration and measurement planes

Sample preparation and measurements

Test samples can be prepared from any reasonably fine-grained soil or from any liquid that does not chemically interact with the sample holder and/or center conductor. Each soil sample should normally be made as homogeneous as possible by drying, pulverizing, and mixing thoroughly. Samples should then be taken to determine the usual engineering properties of grain-size distribution and plasticity indices.

The normal measurement procedure for solid/liquid mixtures is the following:

a. Lower the temperature of the heat source/sink to the lowest value desired.

b. Carefully weigh the dry, empty sample holder.

c. The sample holder should be filled with a nearly saturated sample of the mixture that has been prepared in an appropriate container (for soil/water mixtures, resealable plastic bags were found to be convenient). The holder can be tapped against a flat, hard surface to uniformly settle the sample.

d. The sample and holder should be carefully weighed, then sealed and connected to the measurement system.

e. The measurement program containing the dielectric property calculation algorithm should then be executed, which will cause the frequency range for the dual directional coupler being used to be stepped through and calculations of ε' and ε'' made.

f. The temperature of the sample can then be increased and the measurement program executed again. For each new temperature setting, the sample should be given at least 10 min to reach equilibrium once the bath has reached the desired setting. The 10-min wait was found experimentally to be more than adequate for sample equilibrium to be achieved.

g. At the end of any particular measurement, the holder cover should be loosened to provide a better opportunity for the sample to dry out. The sample and holder should be periodically weighed to determine approximate values of moisture content. When the sample is thought to be at about the desired volumetric moisture content, the holder should be resealed and reconnected, the sample temperature should be taken back to the lowest desired temperature, and the whole measurement sequence should be repeated.

h. After all measurements have been conducted, the sample should be carefully removed, dried, and weighed to determine its original dry density and to facilitate calculations of volumetric moisture.

3   Sanity Checks

To develop confidence in the experimental procedure, materials were measured whose responses are known experimentally or can be modeled very accurately. These measurements also served to confirm the amount of phase shift required to collapse the calibration and measurement planes as discussed in the previous chapter. Data were collected for empty sample holders, samples of distilled water and ethylene glycol (ethanediol), and a sample of silty soil. Each is discussed in the following sections.

Empty Holder

The first question to answer is "How well does this experimental procedure measure the properties of air?" Ideally, the real part of the complex dielectric constant for dry air should be unity, and the imaginary part should be zero. Figure 5 shows the results of measuring empty sample holders. Considering all of the experimental variables that could have an impact on any measurement such as measurement system drift, connector and connection variability, outer conductor discontinuities created by the sample holder cover, etc., the agreement of empty holder (air) measurements with theoretical predictions is quite remarkable.

The vertical dashed line at 2 GHz separates measurements made in two different frequency ranges. A single dual directional coupler (Figure 1) that covers the entire 50 MHz - 26.5 GHz frequency range that is available from the source does not exist. Two different couplers were used whose ranges of operation overlapped at 2 GHz.

The anomalous behavior centered about 3.75 GHz and 7.5 GHz is associated with the mathematical solution technique. At 3.75 GHz, the empty sample holder should be spanned by about a half of a wavelength; at 7.5 GHz, it should hold about a full wavelength, and so on. The number of wavelengths contained within the sample holder for a material with no loss is proportional to $(\omega d\sqrt{\epsilon}/c$ or the cosine function argument in Equation 16. A half wavelength in the sample holder will result in the complex vector representing the right-hand side of Equation 16 approaching the negative real axis in complex space. A full wavelength corresponds to the vector having made a

complete revolution in complex space and approaching the positive real axis But these two conditions are branch cuts for the $\cos^{-1}(z)$ function and are. therefore, inherently unstable. It has been recently discovered that other researchers have experienced this anomalous behavior and that at least one alternative solution technique has been successfully developed (Baker-Jarvis, Vanzura, and Kissick 1990). Future improvements to the measurement and calculation scheme reported herein will probably include one or more of these alternative solutions.

Much of the data that follow in this chapter show the same anomalous behavior whenever integer multiples of half wavelengths exist within the sample holders. The severity of these peaks decreases with increasing frequency, because at low frequencies the computation of ϵ from Equation 16 involves a division by very small numbers. Any inaccuracies are amplified at low frequencies (<1 GHz). This fact also had a negative impact on low-frequency measurement calibrations. Instrumentation drift was often enough to ruin a calibration at the lowest frequencies in just a few hours. Better measurement equipment (namely, an S-parameter test set and a high-quality set of cables and connectors) would help alleviate this low-frequency measurement problem.

Water

Measured values of the complex dielectric constant for samples of distilled, deionized water are shown in Figure 6. For comparison, Ray's (1972) empirical fits to a large amount of pure and freshwater data are duplicated here. Several observations are in order. First of all, the comparison of measured data to the accepted standard is quite good (less then 4 percent difference), especially for the imaginary term. The sample holder volume was evidently not completely filled with water because of the fact that the holder cover must be pressed down upon the water meniscus, causing water to be squeezed from the holder in an unpredictable way. It is also possible that some evaporation of the sample took place during the 2- to 3-hr measurement period. Both of these phenomena could account for the lower measured values of ϵ'. The hypothesis that the sample holder was never completely full was supported by weight measurements that indicate the holders were never more than 95 percent full during these tests.

Another observation is that because of the good correlation with idealized data, the impact of higher order modes must be relatively small as one would expect (Stratton 1941). As pointed out at Equation 2, higher order transverse modes should appear above 2.3 GHz for pure water, but these data that extend to 4 to 5 GHz continue to behave well. (Water data are cut off at 4 to 5 GHz because the noise floor of the network analyzer measurement system was reached.) The same anomalies observed at half-wavelength intervals in the empty holders also occur in the water with very little impact being observed beyond one and a half wavelengths.
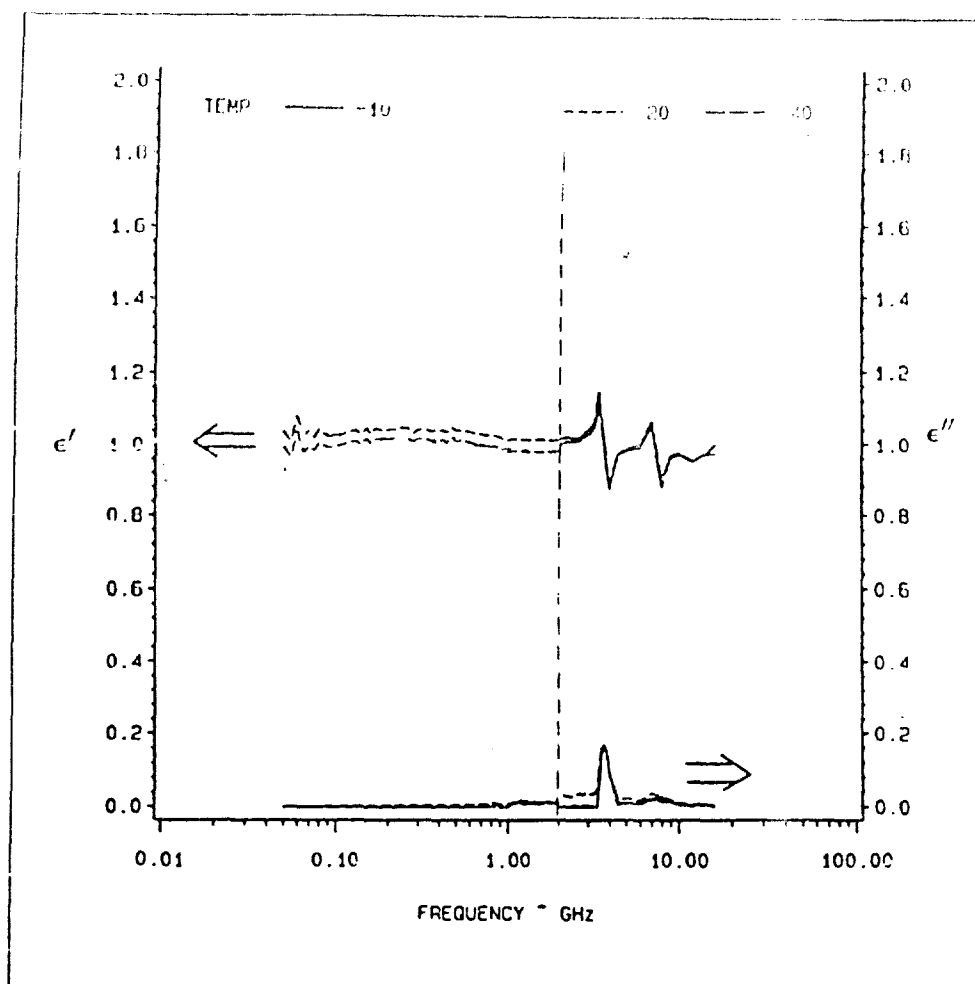
Figure 5. Empty sample holder measurements

The low-frequency tail on ϵ^* may possibly be associated with the ionic conductivity loss mechanism as a result of either trace quantities of ions that escape the deionization process or as a result of ions that originate from unclean and/or oxydized outer or inner conductor surfaces. The magnitude of low-frequency losses are approximately those associated with freshwater conductivity, but the actual loss mechanism has to be viewed as purely speculative.

Ethylene Glycol

Data were collected on several different alcohols: ethylene glycol (ethanediol), methanol, and ethanol. However, because of surface tension problems and rapid evaporation rates, only the results for ethylene glycol ($HOCH_2CH_2OH$, molecular weight 62.07, specific gravity 1.1088 at 20 °C relative to water at 4 °C, <.05 percent water) are reproduced here (Figure 7). Measured values of both $\epsilon^{'}$ and ϵ^{*} are consistently lower than Jordan's (Jordan, Sheppard, and Szwarnowski 1978) results for frequencies greater
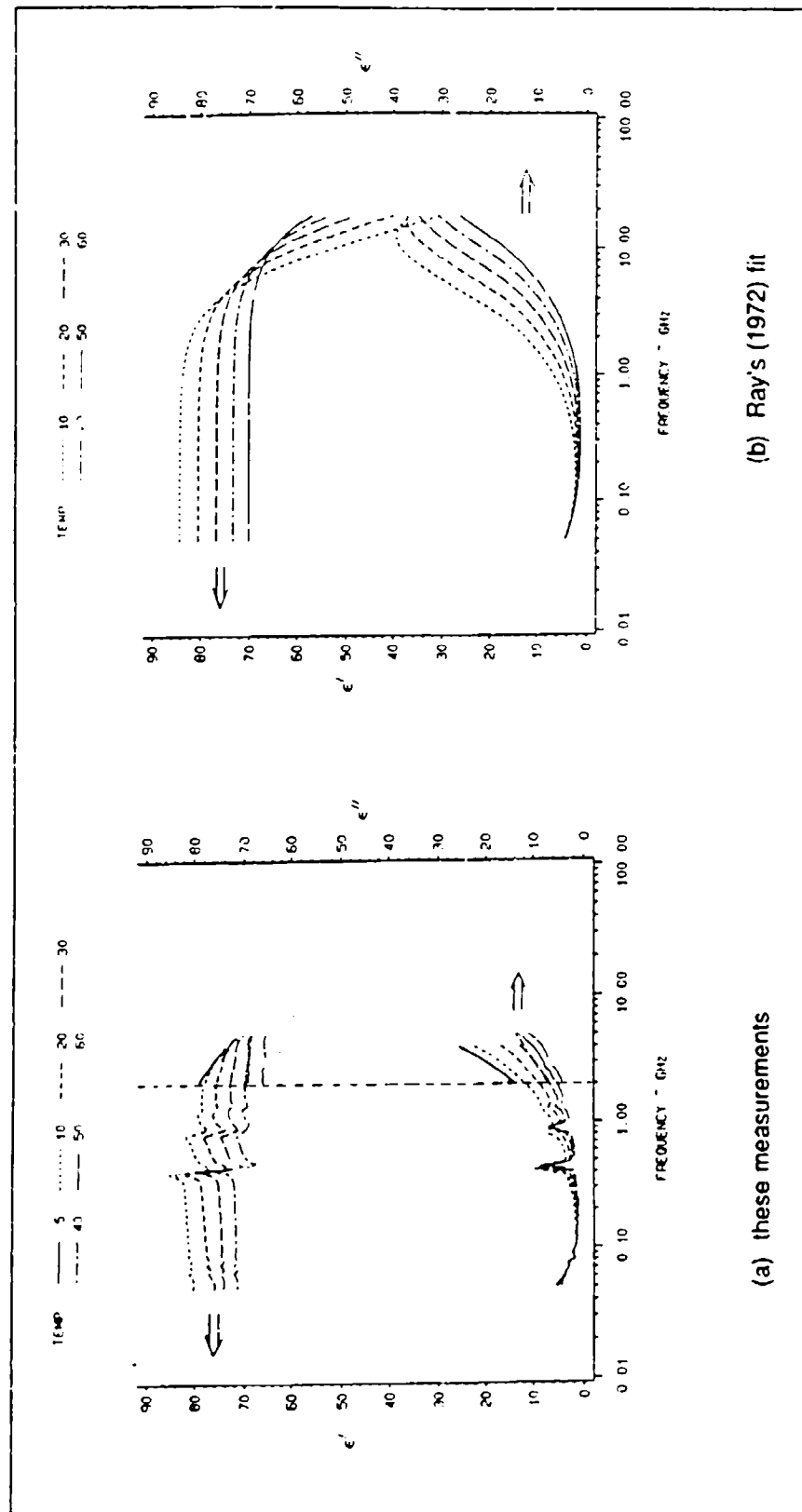
Figure 6   Dispersion curves for water

(a) these measurements

(b) Ray's (1972) fit

Figure 7. Dispersion measurements of ethylene glycol (Continued)
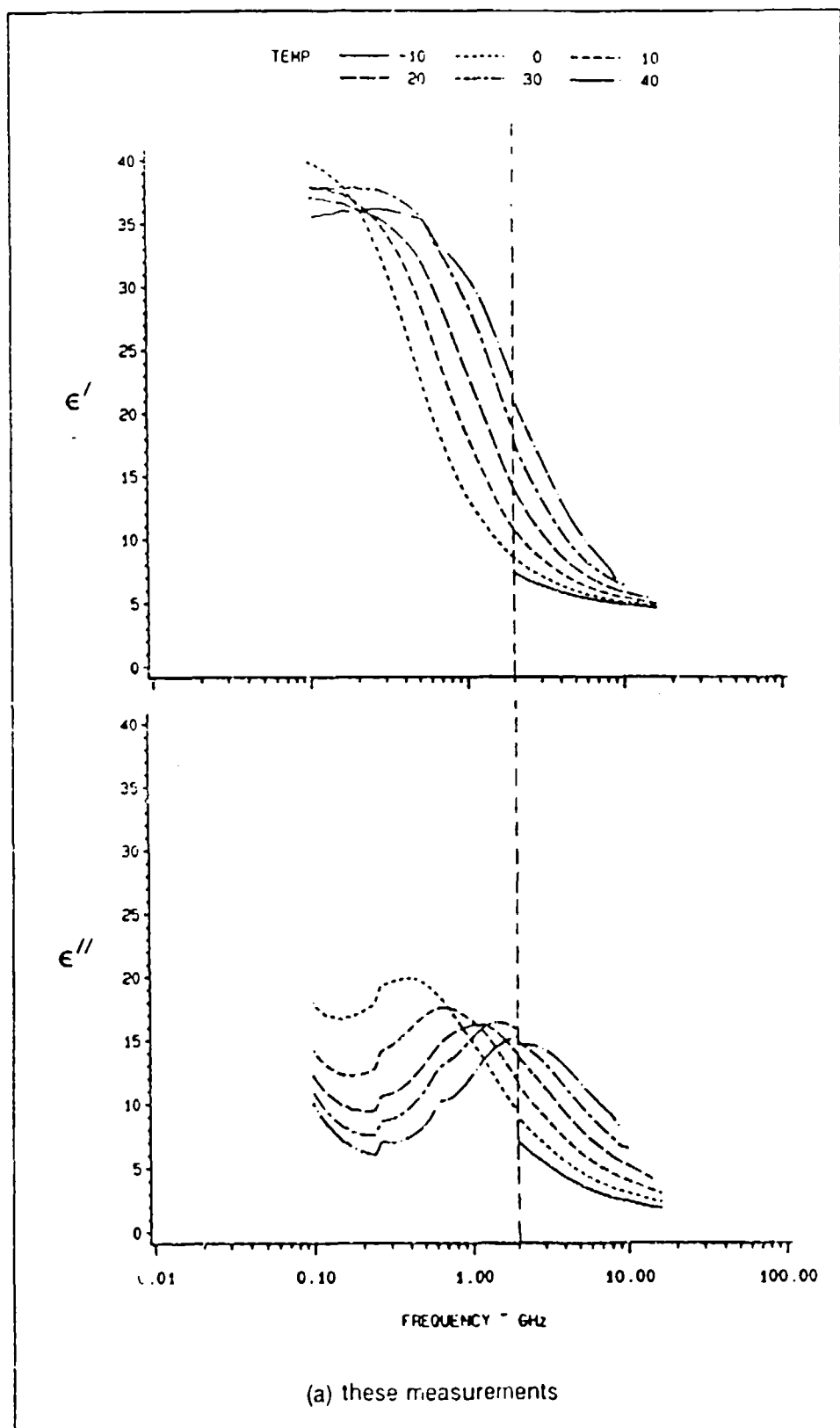
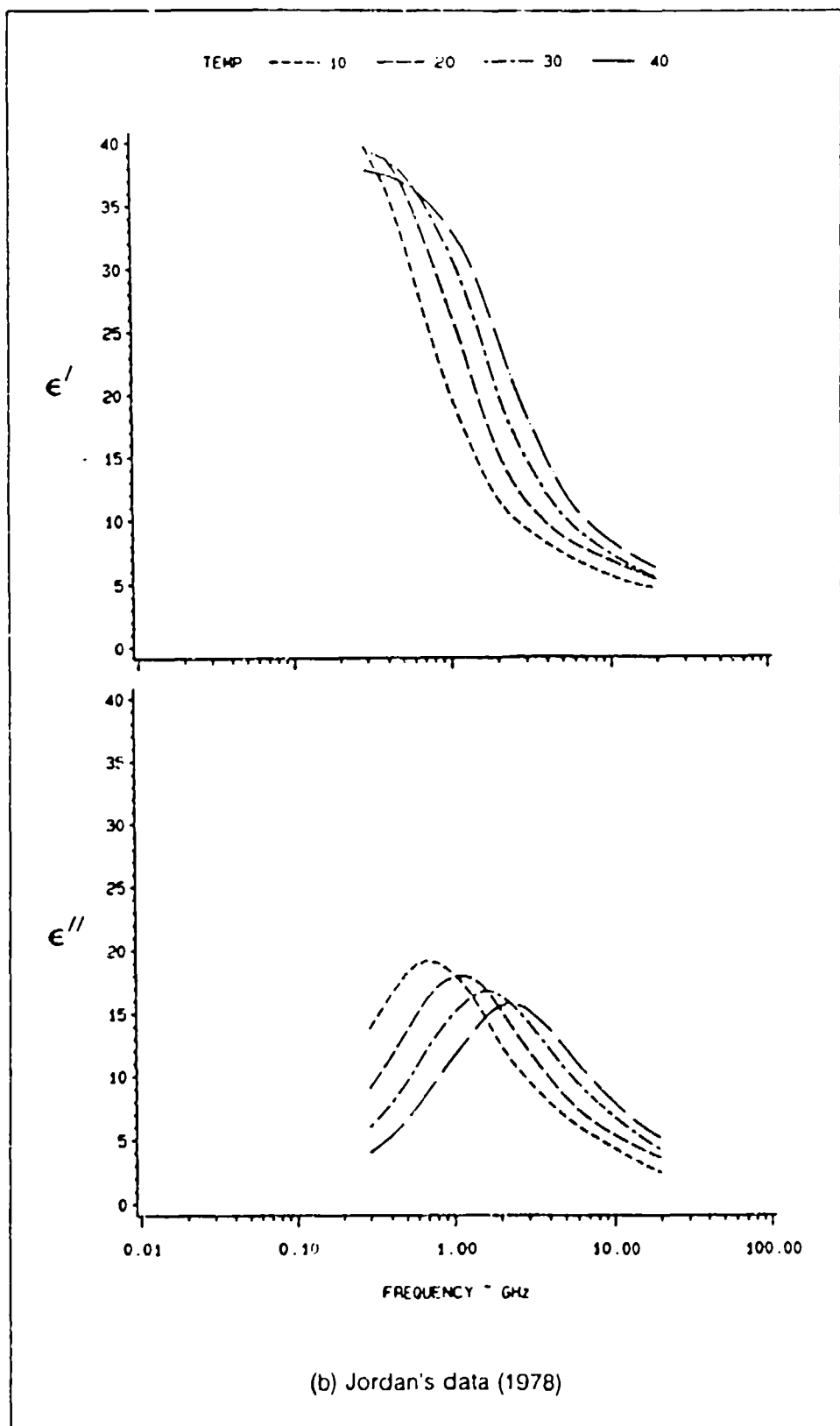Chapter 3 Sanity Checks

(b) Jordan's data (1978)

Figure 7. (Concluded)

than 1 GHz. This is not a surprising observation in that the experimental procedure does suffer from the shortcoming that it is difficult to completely fill the sample holder volume with liquids because of surface tension problems, and it is difficult to maintain the volume of liquid during the 2- to 3-hr measurement period because of evaporation. Although ethanediol was least affected by these problems, sample weights for the high-frequency measurements indicate that the holder was 90 to 95 percent full during the experiments. At low frequencies, measurements revealed another loss mechanism, most likely ionic conductivity.

In summary, results of measurements of air, water, and ethylene glycol are quite good, resulting in a high degree of confidence in the experimental procedure. Differences between these measurements and more precise measurements reported in the literature can be explained by physical and/or chemical factors. One must conclude, however, that improvements would have to be made to the experimental procedure before it could be used to accurately measure the electrical properties of a variety of fluids. In particular, it would be necessary to find a way to completely fill the sample holder and to maintain that fluid level throughout the measurements. The only current concerns with measurements of heterogeneous mixtures of soil and water are cleanliness of the sample holder and uneven drying of the sample throughout its volume.

A Silty Soil

As an example of how data can look for heterogeneous mixtures such as a moist soil, consider the data shown on Figure 8. These data, representing two volumetric moisture content extremes (11.7 and 43.8 percent), are from measurements made at 20 °C on a sample of very clean and somewhat poorly graded silt. More information on the properties of this soil will be available in the third report of this series.

The results of these measurements are certainly sensible. For example, the real part of the complex dielectric constant should be less than that of pure water, as shown in the previous figure. At the same time, the loss term should contain evidence of the relaxation peak beyond 10 GHz, which it does, and should reveal a much greater direct current conductivity contribution below 1 GHz because of the soil chemistry and the formation of free ions in the soil/water mixture.
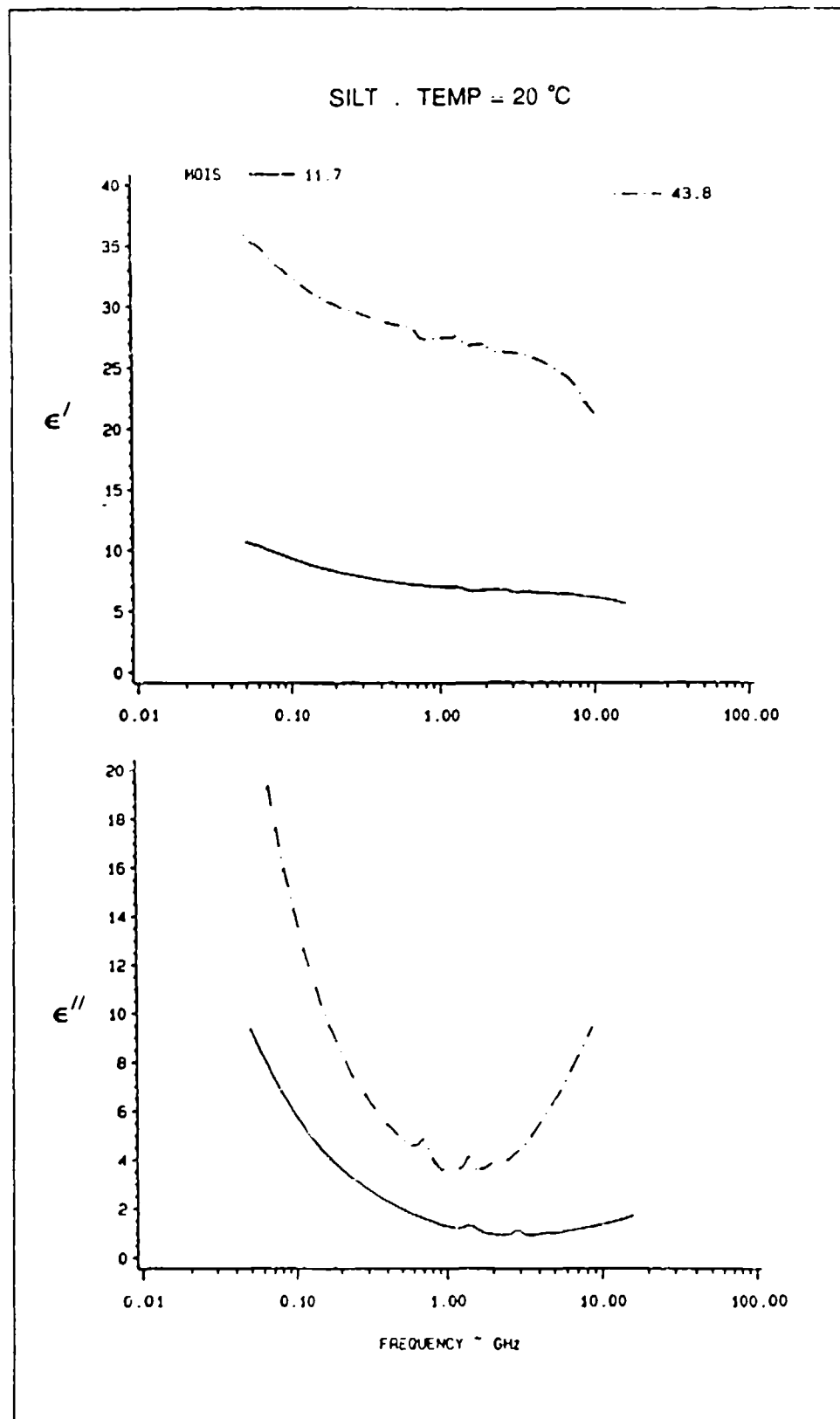
Figure 8   Preliminary dispersion measurements in a silty soil

4 Summary

The response of moist soils (or any other moist heterogeneous mixture) to active microwave sensors is controlled by surface geometry and the dielectric properties of the medium. A review of the literature reveals that what data do exist on dielectric properties suffer from a number of shortcomings. In most cases, the soils are simply not properly characterized in terms of their physical parameters such as the distribution of particle sizes, the dry density under which tests were conducted, or the temperature of the soil, all of which have some impact on the dielectric properties. The volumetric moisture content of the soil, which is usually the most important factor controlling dielectric response, is often not specified or is not computable. And, finally, the data are usually collected at a limited number of frequency values.

In an effort to supplement those data on the complex dielectric properties of moist soils that have been adequately documented, a coaxial measurement apparatus was fabricated to allow electrical property measurements in nominally moist soils to frequencies above 10 GHz. Sample temperatures were controlled by an external bath. The algorithm used to calculate the dispersive complex dielectric constant was verified by measuring the response of liquids whose properties are well documented and the response of air (empty sample holder).

References

Albrecht, H. J. (1966). "Climatic influence upon skin depth in earth." *Proceedings of the IEEE (Correspondence)*.

Arulanandan, K., and Smith, S. S. (1973). "Electrical dispersion in relation to soil structure," ASCE, *Journal of the Soil Mechanics and Foundations Division* SM12, 1113-1133.

Baker-Jarvis, J., Vanzura, E. J., Kissick, W. A. (1990). "Improved technique for determining complex permittivity with the transmission/reflection method." *IEEE Transactions on Microwave Theory and Techniques* 38(8), 1096-1103.

Ballard, R. F. (1983). "Cavity detection and delineation research; Report 5, Electromagnetic (radar) techniques applied to cavity detection," Technical Report GL-83-1, U.S. Army Engineer Waterways Experiment Station, Vicksburg, MS.

Berlin, G. L., Tarabzouni, M. A., Al-Naser, A. H., Sheikho, K. M., and Larson, R. W. (1986). "SIR-B subsurface imaging of a sand-buried landscape: Al Labbah Plateau, Saudi Arabia." *IEEE transactions on geoscience and remote sensing*. GE-24(4), 595-602.

Birchak, J. R., Gardner, C. G., Hipp, J. E., and Victor, J. M. (1974). "High dielectric constant microwave probes for sensing soil moisture." *Proceedings of the IEEE* 62(1), 93-98.

Brunfeldt, D. R. (1987). "Theory and design of a field-portable dielectric measurement system." *Proceedings of IGARSS '87 Symposium*. Ann Arbor, MI, 559-563.

Campbell, J. E. (1988). "Dielectric properties of moist soils at RF and microwave frequencies," Ph.D. diss., Dartmouth College, Hanover, NH.

_____. (1990). Unpublished laboratory studies conducted at Dartmouth College, Hanover, NH.

Campbell, M. J., and Ulrichs, J. (1969). "Electrical properties of rocks and their significance for lunar radar observations." *Journal of Geophysical Research* 74(25), 5867-5881.

Colwell, R. N., ed. (1983). *Manual of remote sensing*. 2nd ed., American Society of Photogrammetry, Falls Church, VA.

Curtis, (1992). "Moisture and temperature effects on the microwave dielectric behavior of soils," Ph.D. diss., Dartmouth College, Hanover, NH.

_____. "Microwave dielectric behavior of soils; Report 1, Summary of related research and applications," Technical Report in preparation, U.S. Army Engineer Waterways Experiment Station, Vicksburg, MS.

Farr, T. G., Elachi, C., Hartl, P., and Chowdhury, K. (1986). "Microwave penetration and attenuation in desert soil." *IEEE transactions on geoscience and remote sensing*. GE-24(4), 590-594.

Gabriel, C., Grant, E. H., and Young, I. R. (1986). "Use of time domain spectroscopy for measuring dielectric properties with a coaxial probe," *Journal of Physics, E: Scientific Instrumentation* 19, 843-846.

Hayre, H. S. (1970). "Geophysical dielectric constant determination." *IEEE transactions on geoscience electronics*. GE-8(4), 289-295.

Hewlett-Packard Company. (1985). "Materials measurement," Product Note 8510-3, Santa Rosa, CA.

_____. (1991). *Operating and programming manual, HP 8510C Network Analyzer*. Santa Rosa, CA.

Hippel, A. R. von. (1954). *Dielectrics and Waves*. John Wiley and Sons, Inc., New York.

Hoekstra, P., and Delaney, A. (1974). "Dielectric properties of soils at UHF and microwave frequencies," *Journal of Geophysical Research* 79(11), 1699-1708.

Jakkula, P., Ylinen, P., and Tiuri, M. (1980). "Measurement of ice and frost thickness with an FM-CW radar." *Proceedings of the 10th European microwave conference*. Warszawa, Poland, 584-587.

John, B. (1992). "Soil moisture detection with airborne passive and active microwave sensors," *International Journal of Remote Sensing* 13(3), 481-491.

Jordan, B. P., Sheppard, R. J., and Szwarnowski, S. (1978). "The dielectric properties of formamide, ethanediol and methanol," *Journal of Physics D*. 11, 695-701.

Lundien, J. R. (1966). "Terrain analysis by electromagnetic means; Report 2, Radar responses to laboratory prepared soil samples," TR 3-693, U.S. Army Engineer Waterways Experiment Station, Vicksburg, MS.

_____. (1972). "Determining presence, thickness, and electrical properties of stratified media using swept-frequency radar," TR M-72-4, U.S. Army Engineer Waterways Experiment Station, Vicksburg, MS.

Madden, T. R. (1974). "Near surface electrical properties of rocks as a guide to mechanical properties," Report AFCRL-TR-75-0179, Air Force Cambridge Research Laboratories, Hanscom, AFB, MA.

McCauley, J. F., Breed, C. S., Schaber, G. G., McHugh, W. P., Issawi, B., Haynes, C. V., Grolier, M. J., and el Kilani, A. (1986). "Paleodrainages of the Eastern Sahara - The Radar Rivers Revisited (SIR-A/B Implications for a Mid-Tertiary Trans-African Drainage System." *IEEE transactions on geoscience and remote sensing.* GE-24(4), 624-648.

Nelson, S. O. (1973). "Microwave dielectric properties of grain and seed." *Transactions of the ASAE.* 16(5), 902-905.

_____. (1983). "Dielectric properties of some fresh fruits and vegetables at frequencies of 2.45 to 22 GHz." *Transactions of the ASAE.* 26(2), 613-616.

Olhoeft, G. R. (1983). "Impulse radar studies of near surface geological structure." *Proceedings of the conference on lunar and planetary science X,* Houston, TX, 943-945.

O'Neill, K., and Arcone, S. A. (1991). "Investigations of freshwater and ice surveying using short-pulse radar," CRREL Report 91-15, U.S. Army Engineer Cold Regions Research and Engineering Laboratory, Hanover, NH.

Parchomchuk, P., Wallender, W. W., and King, R. J. (1990). "Calibration of a waveguide sensor for measuring soil moisture." *IEEE transactions on geoscience and remote sensing.* 28(5), 873-878.

Ray, P. S. (1972). "Broadband complex refractive indices of ice and water," *Applied Optics* 11(8), 1836-1844.

Schaber, G. G., McCauley, J. F., Breed, C. S., and Olhoeft, G. R. (1986). "Shuttle imaging radar: Physical controls on signal penetration and subsurface scattering in the Eastern Sahara." *IEEE transactions on geoscience and remote sensing.* GE-24(4), 603-62

Stewart, M. T. (1982). "Evaluation of electromagn ic methods for rapid mapping of salt-water interfaces in coastal aqui s," *Ground Water* 20(5), 538-545.

Stratton, J. A. (1941). *Electromagnetic theory*. McGraw-Hill Book Co., New York.

Swanson, R., Zoughi, R., Moore, R. K., Dellwig, L. F., and Soofi, A. K. (1988). "Backscatter and dielectric measurements from rocks of southeastern Utah at C-, X-, and K$_u$- Bands." *International Journal of Remote Sensing* 9(4), 625-639.

Taherian, M. R., Yuen, D. J., Habashy, T. M., and Kong, J. A. (1991). "A coaxial-circular waveguide for dielectric measurement." *IEEE transactions on geoscience and remote sensing*. 29(2), 321-330.

Telford, W. M., Geldart, L. P., Sheriff, R. E., and Keys, D. A. (1984). "Electrical properties of rocks." *Applied geophysics*. Chapter 5, Cambridge University Press.

Thomas, A. M. (1966). "In situ measurement of moisture in soil and similar substances by fringe capacitance." *Journal of Scientific Instruments* 43, 21-27.

Topp, G. C., Davis, J. L., Annan, A. P. (1980). "Electromagnetic determination of soil water content: Measurements in coaxial transmission lines." *Water Resources Research* 16(3), 574-582.

Ulaby, F. T., Cihlar, J., and Moore, R. K. (1974). "Active microwave measurement of soil water content." *Remote Sensing of Environment* 3, 185-203.

Wegmuller, Urs. (1990). "The effect of freezing and thawing on the microwave signatures of bare soil." *Remote Sensing of the Environment* 33, 123-135.

Wright, D. L., Olhoeft, G. R., and Watts, R. D. (1984). "Ground-penetrating radar studies on Cape Cod." *Proceedings of NWWA/EPA conference on surface and borehole geophysical methods in ground water investigations*. San Antonio, TX, 666-681.

Zucker R. (1972). "Elementary transcendental functions." *Handbook of mathematical functions with formulas, graphs, and mathematical tables*. M. Abramowitz and I. A. Stegun, ed., 10th printing, U.S. Government Printing Office, Washington, DC.

References

Appendix A
Skin Depth Calculations

Obviously, skin depth effects preclude the utility of practical electromagnetic devices to penetrate to distances comparable with acoustic devices, but nevertheless, low-frequency devices have some utility (Berlin et al. 1986; Farr et al. 1986; Schaber et al. 1986).[1] As a means of quantifying the penetration of electromagnetic waves into earth media in terms of the complex dielectric constant of the media, one should consider the following arguments. The one-dimensional propagation of an electromagnetic wave into some medium can be described by an amplitude function such as

$$e^{i(kx - \omega t)} \tag{A1}$$

where

i = symbol designating the imaginary quantity $\sqrt{-1}$

k = complex wave number

x = distance

ω = radial frequency

t = time

Furthermore, let

$$k \equiv \beta + i \frac{\alpha}{2} \tag{A2}$$

---

[1] References cited in this appendix are located at the end of the main text.

where

β = phase constant and governs how a lossless medium propagates a wave

α = attenuation factor and controls how the amplitude of the wave decreases with distance traveled through the medium

Then the amplitude of the wave is

$$e^{i(\beta x - \omega t)} e^{-\left(\frac{\alpha}{2}\right)x} \tag{A3}$$

i.e., a traveling wave combined with an attenuation factor.

If skin depth is defined as that distance over which the wave amplitude decreases by a factor of $1/e$, then the skin depth δ is

$$\delta \equiv \frac{2}{\alpha} \tag{A4}$$

But the wave number can also be written

$$k = \frac{\omega}{v} = \frac{\omega N}{c} \tag{A5}$$

where

v = phase velocity in the medium

c = speed of light

N = complex index of refraction
  = $n' + in''$

Thus

$$\delta = \frac{2}{\alpha} = \frac{c}{\omega n''} \tag{A6}$$

or the skin depth is inversely proportional to the imaginary part of the complex index of refraction.

However, this study focuses on the complex dielectric constant ε as the measure of soil electrical characteristics.

A2

$$\varepsilon = \varepsilon' + i\varepsilon'' \equiv N^2 \tag{A7}$$

Following several substitutions and simplifications, one can show that

$$\delta = \frac{\lambda_0}{2\pi} \left[\varepsilon' \frac{\left(\sqrt{1 + (\varepsilon''/\varepsilon')^2} - 1 \right)}{2} \right]^{-\frac{1}{2}} \tag{A8}$$

where λ_0 is the free-space wavelength. A visualization of this equation for the range of values of permittivity ε' and loss tangent $\varepsilon''/\varepsilon'$ normally found in soils is provided in Figure A1. This figure does not represent any new science, as the same information has been presented in other forms (von Hippel 1954). It is, however, a more condensed way of visualizing the skin depth that has not been observed elsewhere in the literature. Figure A1 is valid for any interpretation of loss tangent; i.e., whether one is speaking of a loss mechanism because of actual charge migration or one because of dielectric relaxation.

Another useful skin depth relationship found in the literature is the nomograph generated by Albrecht (1966) and reproduced on Figure A2. Albrecht first developed an empirical relationship that associated ground conductivity to gravimetric moisture content and ground temperature at low frequencies. He then related skin depth to wavelength and conductivity by the usual equation for highly conductive materials (assumes that the conductivity phenomenon dominates the loss mechanism in soils at low frequencies):

$$\delta = \sqrt{\frac{\lambda_o}{\pi \mu c \sigma}} \tag{A9}$$

where the units used are MKS, and the skin depth is in meters and the ground conductivity is in units of mho/meter. The magnetic permeability was taken to be $4\pi \times 10^7$ Henrys/meter. The way to use this nomograph is to select a moisture content and move on a horizontal line to the appropriate temperature curve. Then move on a vertical line to the appropriate frequency curve. From that point, a horizontal line to the right-hand scale reveals the desired value of skin depth. There is no way to relate Albrecht's results to those of Figure A1, because it begins with an unknown empirical relationship among moisture, temperature, and conductivity.

Hoekstra and Delaney (1974) also published some useful data on plane wave attenuation in moist soils at higher frequencies. These data are shown in Figure A3. They concluded that attenuation was relatively independent of soil fabric and that either passive or active microwave sensors could obtain a measurable response from only about the first 5 cm of ground below the surface.
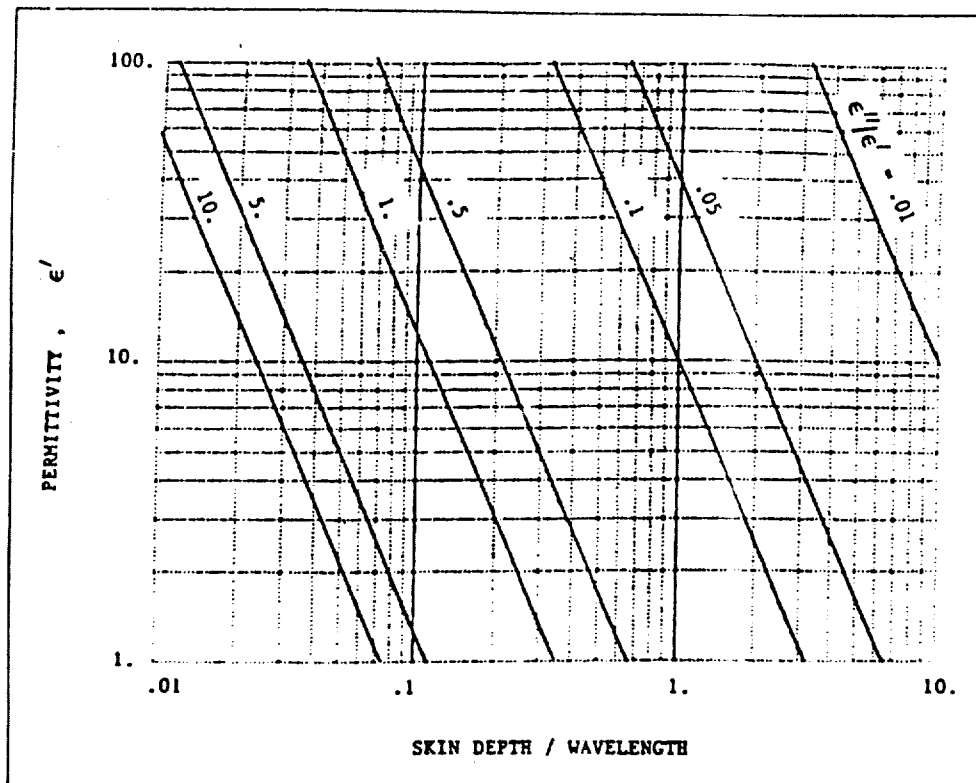
Figure A1. Skin depth as a function of wavelength, permittivity, and loss tangent

Figure A2   Skin depth nomograph (from Albrecht (1966))
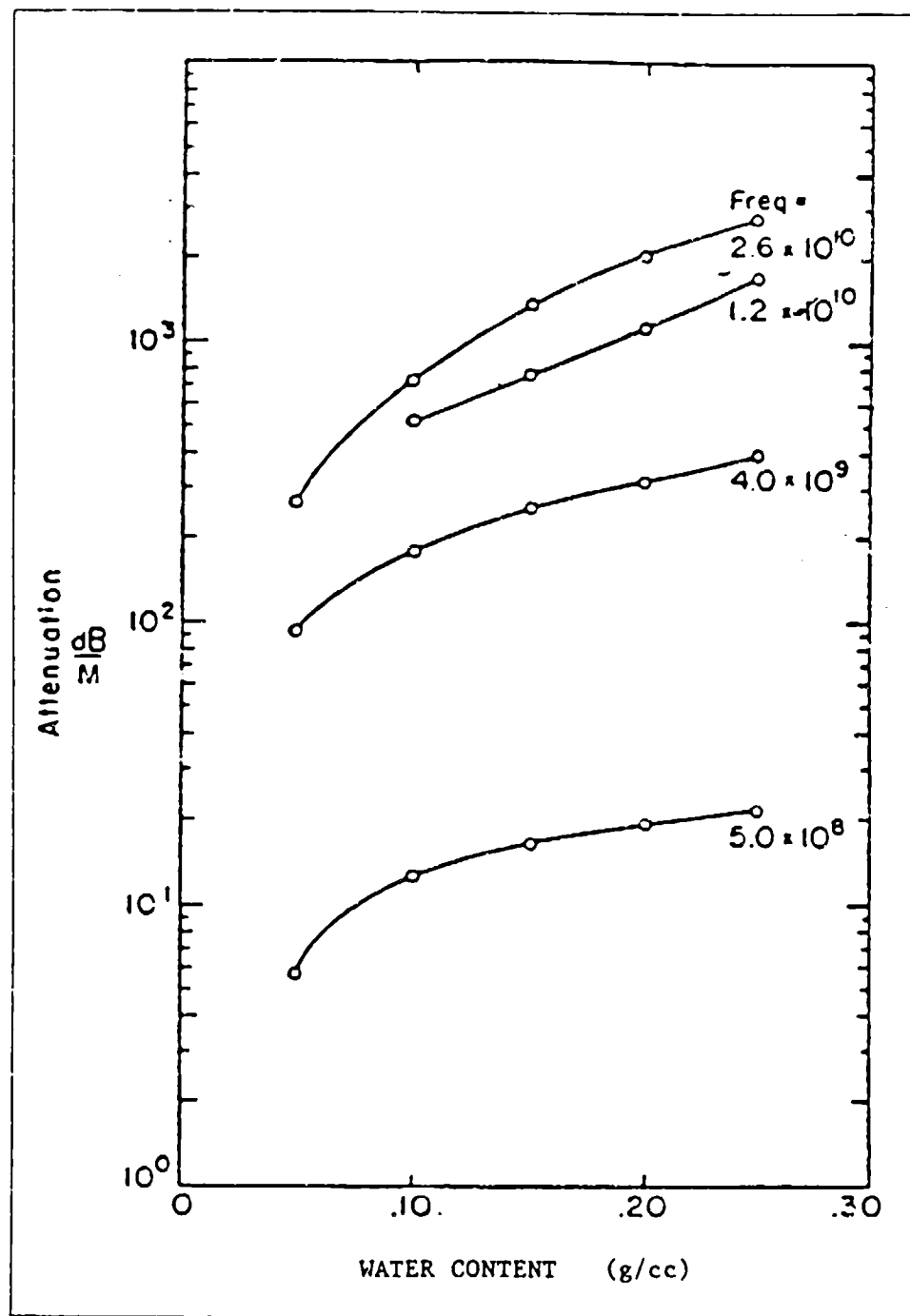
Figure A3. Attenuation in moist soils (from Hoekstra and Delaney (1974))

Appendix B
Program Listing and Sample Output

The following program, written in the HP BASIC language and executed in an interactive mode on an HP9000 Series 360 system controller, drives the vector network analyzer-based system used to collect complex reflection/transmission parameters, store those data on permanent files, and generate a real-time hard copy output of calculated complex dielectric constant values. An example output sheet is also included.

```
10    !   PROGRAM NAME:  EPSILONS
11    !
12    !   A MULTIPURPOSE CODE FOR   1) COLLECTING COAXIAL REFLECTION AND
13    !   TRANSMISSION DATA AND CALCULATING BOTH THE REAL AND IMAGINARY
14    !   PARTS OF THE COMPLEX DIELECTRIC CONSTANT, OR   2) DISPLAYING
15    !   THE RESULTS OF PREVIOUSLY COLLECTED DATA
16    !
17    !   THE HIGH FREQUENCY OPTION USES AN HP11692D DIRECTIONAL COUPLER
18    !   AND COVERS THE 1.5-17.5 GHz RANGE.
19    !
20    !   THE LOW FREQUENCY OPTION USES AN HP778D DIRECTIONAL COUPLER
21    !   AND COVERS THE 45 MHz TO 2.045 GHz RANGE.
23    !
24    !   USES THE HP9000 ACS ALGORITHM WITH SIGN ADJUSTMENTS
25    !
26    OPTION BASE 1
30    COMPLEX S11(1:801),S21(1:801),Rhs,Lhs,Rt,Eps
40    INTEGER Preamble,Bytes,Phscorr
41    REAL Binary(1:801,1:2)
50    DIM Ttl$[60],Secline$[60],Epsp(1:801),Epspp(1:801)
60    ASSIGN @Nwa TO 716
70    ASSIGN @Nwa_data TO 716;FORMAT OFF
80    LOCAL @Nwa
90    PRINTER IS CRT
100   GINIT
110   PLOTTER IS CRT,"INTERNAL"
120   GRAPHICS ON
130   Fd$=DATE$(TIMEDATE)
131   Ft$=TIME$(TIMEDATE)
150   CLEAR SCREEN
160   PRINT Fd$,Ft$                                    ! DATE AND TIME AT BEGINNING
OF MEASUREMENT
170   BEEP 4000,.2
171   D=4
173   PRINT
174   PRINT "INSTRUMENT STATE 1 IS ASSOCIATED WITH THE HIGH FREQUENCY COUPLER"
175   PRINT "INSTRUMENT STATE 2 IS ASSOCIATED WITH THE LOW FREQUENCY COUPLER"
176   PRINT
177   INPUT "WHICH INSTRUMENT STATE DO YOU WANT TO USE?",N1
179   Fi=4.5E+7
180   Ff=2.045E+9
181   Np=401
182   IF N1=2 THEN GOTO 190
183   Fi=1.5E+9
184   Ff=1.75E+10
185   Np=801
189   !
190   ASSIGN @Hpib TO 7
191   REMOTE @Hpib
192   ABORT @Hpib
193   CLEAR @Nwa
194   CLEAR 717
196   OUTPUT @Nwa;"WAIT;RECA"&VAL$(N1)&";"            ! RECALL INSTRUMENT STAT
E
197   OUTPUT @Nwa;"WAIT;CHAN1;WAIT;S12;LOCKA1;NUMEB2;DENOA1;REDD;"   ! REDEFINE S
12 & S22 BECAUSEA 1-PATH, 2-PORT CAL IS BEING USED
198   OUTPUT @Nwa;"WAIT;S22;LOCKA1;NUMEB1;DENOA1;REDD;"
199   OUTPUT @Nwa;"WAIT;S11;"
200   OUTPUT @Nwa;"CALS"&VAL$(N1)&";"                 ! RECALL CAL SET
```

```
201    OUTPUT @Nwa;"WAIT;PRINTYPECOLR;"              ! PRINT COLORS
202    BEEP 4000,.2
203    PRINT
204    INPUT "ARE YOU COLLECTING NEW DATA (1) OR RESTORING AN EXISTING FILE (2)?
,Ndf
205    IF Ndf=1 THEN GOTO 246
206    !
207    !  RETRIEVE AN EXISTING DATA FILE FOR FURTHER ANALYSIS
208    !
209    BEEP 4000,.2
210     PRINT
211     PRINT "PREPARE FOR A DUMMY MEASUREMENT TO PROPERLY RESET THE INSTRUMENT :
TATE"
212     PRINT "WHEN YOU ARE READY, PRESS THE 'CONTINUE' KEY"
213     PAUSE
214     Wtime=80
215     IF Ni=2 THEN Wtime=62
216     OUTPUT @Nwa;"SING;"
217     WAIT 3
218     TRIGGER @Nwa
219     WAIT Wtime !  TIME REQUIRED FOR A SWEEP WITH AVERAGING
220     TRIGGER @Nwa
221     WAIT Wtime
222    BEEP 4000,.2
223    PRINT
224    INPUT "WHAT IS THE NAME OF THE EXISTING DATA FILE?",Namef$
225    ASSIGN @F1 TO "DISSDATA/"&Namef$;FORMAT OFF
226    OUTPUT @Nwa;"CHAN1;FORM3;INPURAW1;"
227    ENTER @F1;Preamble;Bytes
228    M=Bytes/16
229    PRINT "NUMBER OF DATA POINTS IN FILE=",M
230    REDIM Binary(1:M,1:2)
231    REDIM S11(1:M),S21(1:M)
232    ENTER @F1;Binary(*)
233    OUTPUT @Nwa_data;Preamble,Bytes,Binary(*)
238    OUTPUT @Nwa;"WAIT;CHAN2;FORM3;INPURAW2;"
239    ENTER @F1;Preamble;Bytes;Binary(*)
240    OUTPUT @Nwa_data;Preamble;Bytes;Binary(*)
241    ASSIGN @F1 TO *
242    GOTO 302
243    !
244    !  PREPARE TO MAKE A NEW SET OF MEASUREMENTS
245    !
246    OUTPUT @Nwa;"OPEP;"
263    Namef$=Fd$[1,2]&Fd$[4,6]&Fd$[11,11]&Ft$[1,2]&Ft$[4,5]
264    PRINT
265    PRINT "THE BINARY DAT FILE NAME IS ",Namef$
266    IF Ni=1 THEN GOTO 270
267    CREATE BDAT "/DISSDATA/"&Namef$,1,6448              ! CREATE DATA FILE
268    GOTO 271
270    CREATE BDAT "/DISSDATA/"&Namef$,1,12848             ! CREATE DATA FILE
271    ASSIGN @F1 TO "/DISSDATA/"&Namef$;FORMAT OFF
273    Wtime=80
274    IF Ni=2 THEN Wtime=62
275    OUTPUT @Nwa;"SING;"
276    WAIT 3
277    TRIGGER @Nwa
278    WAIT Wtime !  TIME REQUIRED FOR A SWEEP WITH AVERAGING
279    TRIGGER @Nwa
280    WAIT Wtime
```

```
281   !
282   !   STORE A NEW DATA FILE
283   !
284   OUTPUT @Nwa;"CHAN1;FORM3;OUTPRAW1;"
285   ENTER @Nwa_data;Preamble;Bytes
286   M=Bytes/16
287   REDIM Binary(1:M,1:2)
288   REDIM S11(1:M),S21(1:M)
289   ENTER @Nwa_data;Binary(*)
294   OUTPUT @F1;Preamble;Bytes;Binary(*)
295   OUTPUT @Nwa;"WAIT;CHAN2;FORM3;OUTPRAW2;"
296   ENTER @Nwa_data;Preamble;Bytes;Binary(*)
297   OUTPUT @F1;Preamble;Bytes;Binary(*)
298   ASSIGN @F1 TO *
299   !
300   !   DISPLAY REAL,IMAGINARY PAIRS ON A POLAR PLOT
301   !
302   OUTPUT @Nwa;"WAIT;CHAN2;WAIT;REIP;WAIT;AUTO;"
303   OUTPUT @Nwa;"WAIT;CHAN1;WAIT;REIP;WAIT;AUTO;ENTO;"
304   !
311   !
312   !   SELECT DELAY VALUES FOR EITHER OR BOTH CHANNELS
313   !
317   PRINT
318   INPUT "INPUT THE ELECTRICAL DELAY IN PICOSECONDS",Ed
319   OUTPUT @Nwa;"CHAN1;ELED";Ed;"ps;"
320   OUTPUT @Nwa;"CHAN2;ELED";Ed;"ps;ENTO;"
321   !
322   !   ESTIMATE THE INITIAL 'N' VALUE FOR COMPUTING THE CORRECT PHASE ANGLE
323   !
324   OUTPUT @Nwa;"CHAN2;DELA;WAIT;"
325   OUTPUT @Nwa;"MARK1";F1;";"
326   OUTPUT @Nwa;"OUTPMARK;"
327   ENTER @Nwa;Tau,Dummy
328   N=INT(Tau*F1)
329   PRINT "N,TAU ",N,Tau
330   IF N<0 THEN N=0
331   IF N>99 THEN N=99
332   OUTPUT @Nwa;"WAIT;REIP;WAIT;AUTO;"
334   !
335   !    LOAD THE DATA INTO COMPLEX ARRAYS ON THE 330 FOR FURTHER PROCESSING
336   !
337   OUTPUT @Nwa;"WAIT;CHAN1;FORM3;OUTPFORM;"
338   ENTER @Nwa_data;Preamble;Bytes;S11(*)
339   OUTPUT @Nwa;"WAIT;CHAN2;FORM3;OUTPFORM;"
340   ENTER @Nwa_data;Preamble;Bytes;S21(*)
341   !
342   !   CALCULATE THE COMPLEX DIELECTRIC CONSTANT
343   !
344   BEEP 4000,.2
345   C=3.E+10
346   RAD
347   PRINTER IS CRT
348   LINPUT "DO YOU NEED TO SPECIFY THE NUMBER OF WAVELENGTHS IN THE SAMPLE?",A
wl$
349   IF Awl$="N" THEN GOTO 351
350   INPUT "INPUT THAT NUMBER",N
351   N1st=N
353   Angle1=0.
354   Imrhs=0
```

```
356    INPUT "TEST VALUE FOR IMAG(Rhs) IS 0.0   DO YOU WANT ANOTHER VALUE?",Aim$
357    IF Aim$="N" THEN GOTO 359
358    INPUT "INPUT THE CUTOFF VALUE",Imrhs
359    !
360    FOR I=1 TO Np
361    Rhs=(1+S21(I)*S21(I)-S11(I)*S11(I))/(2*S21(I))
362    IF ABS(Rhs)>1.E+6 THEN GOTO 382
363    IF ABS(IMAG(Rhs))<Imrhs THEN Rhs=CMPLX(REAL(Rhs),0)
364    Lhs=ACS(Rhs)
365    Lhs=CMPLX(REAL(Lhs),ABS(IMAG(Lhs)))
366    IF IMAG(Rhs)<0 THEN Lhs=CMPLX(2*PI-REAL(Lhs),IMAG(Lhs))
367    Angle=REAL(Lhs)
368    IF I=1 THEN GOTO 372
369     IF ABS(Angle-Angle1)<4.5 THEN GOTO 372
371     N=N+1
372     Lhs=CMPLX(REAL(Lhs)+N*2*PI,IMAG(Lhs))
373    ! PRINT USING "DDDD,5(2X,SDDD.DDD),2X,DDD";I,Rhs,Lhs,Angle,N
374     Angle1=Angle
375    Rhs=Lhs*Lhs
376    Radfreq=2*PI*(Fi+(I-1)*(Ff-Fi)/(Np-1))
377    Fact=C/(Radfreq*D)
378    Epsp(I)=Fact*Fact*REAL(Rhs)
379    Epspp(I)=Fact*Fact*IMAG(Rhs)
380    !  PRINT Epsp(I),Epspp(I)
382    NEXT I
383    !
384    !   PLOT THE RESULTS
385    !
386    BEEP 4000,.2
387    GINIT
389    PRINTER IS CRT
390    LINPUT "INPUT A TITLE FOR THE PLOT",Ttl$
391    PRINT
392    PRINT "MAXIMUM VALUE OF EPSP=",MAX(Epsp(*))
393    PRINT
394    PRINT "MAXIMUM VALUE OF EPSPP=",MAX(Epspp(*))
395    PRINT
396    INPUT "INPUT THE MINIMUM AND MAXIMUM VALUES OF EPSILON THAT WILL BE PLOTTE
D",Wmin,Wmax
397    INPUT "INPUT THE TICK MARK INCREMENT IN UNITS OF EPSILON",Ytick
398    CLEAR SCREEN
399    Xmax=100*MAX(1,RATIO)
400    Ymax=100*MAX(1,1/RATIO)
401    LORG 6
402    CSIZE 1.7
403    MOVE Xmax*.3,Ymax
404    LABEL Ttl$
406    Secline$="FILE: "&Namef$&"   N= "&VAL$(N1st)&"   DELAY= "&VAL$(Ed)&" ps"
408    MOVE Xmax*.3,Ymax*.97
409    LABEL Secline$
411    DEG
412    LDIR 90
413    MOVE Xmax*.04,Ymax*.87
414    LABEL "EPS'"
415    MOVE Xmax*.04,Ymax*.67
416    LABEL "EPS''"
417    LORG 4
418    LDIR 0
419    MOVE Xmax*.3,.55*Ymax
420    LABEL "FREQUENCY (GHz)"
```

```
421    VIEWPORT .1*Xmax,.5*Xmax,.8*Ymax,.95*Ymax
422    WINDOW 7,11,Wmin,Wmax
423    AXES 1,Ytick,7,0,1,1,2
424    CLIP OFF
425    CSIZE 1.5,.5
426    LORG 6
427    FOR I=8 TO 11
428    MOVE I,-.2*Ytick
429    LABEL USING "#,K";(10^I)/1.E+9
430    FOR J=2 TO 9
431    Jtick=LGT(J)
432    MOVE I-1+Jtick,Wmin
433    PLOT I-1+Jtick,.04*(Wmax-Wmin),-1
434    NEXT J
436    NEXT I
437    LORG 8
438    FOR I=Wmin TO Wmax STEP Ytick
439    MOVE 6.85,I
440    LABEL USING "#,SDDD.D";I
441    NEXT I
442    PENUP
443    FOR I=1 TO Np
444    IF ABS(Epsp(I))<.001 THEN GOTO 447
445    X=LGT(Pi+(I-1)*(Ff-Fi)/(Np-1))
446    PLOT X,Epsp(I)
447    NEXT I
448    VIEWPORT .1*Xmax,.5*Xmax,.6*Ymax,.75*Ymax
449    WINDOW 7,11,Wmin,Wmax
450    AXES 1,Ytick,7,0,1,1,2
451    CLIP OFF
452    CSIZE 1.5,.5
453    LORG 6
454    FOR I=8 TO 11
455    MOVE I,-.2*Ytick
456    LABEL USING "#,K";10^I/1.E+9
457    FOR J=2 TO 9
458    Jtick=LGT(J)
459    MOVE I-1+Jtick,Wmin
460    PLOT I-1+Jtick,.04*(Wmax-Wmin),-1
461    NEXT J
462    NEXT I
463    LORG 8
464    FOR I=Wmin TO Wmax STEP Ytick
465    MOVE 6.85,I
466    LABEL USING "#,SDDD.D";I
467    NEXT I
468    PENUP
469    FOR I=1 TO Np
470    IF ABS(Epspp(I))<.001 THEN GOTO 473
471    X=LGT(Pi+(I-1)*(Ff-Fi)/(Np-1))
472    PLOT X,Epspp(I)
473    NEXT I
474    KEY LABELS OFF
475    PAUSE
476    CLEAR SCREEN
477    KEY LABELS ON
478    LOCAL @Nwa
479    BEEP 4000,.2
480    !  PRINT
481    !  INPUT "DO YOU WANT TO STORE THIS FILE ON A BACKUP TAPE?",Ans$
```
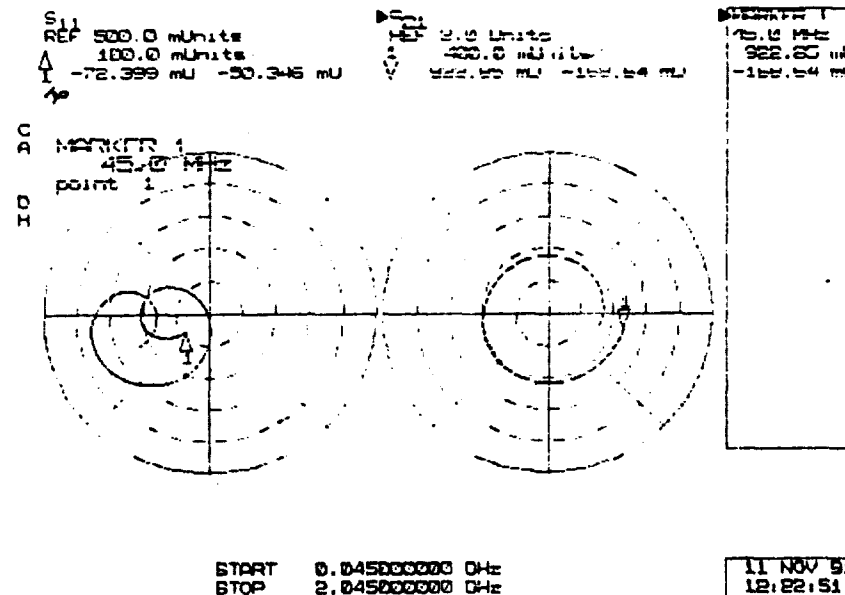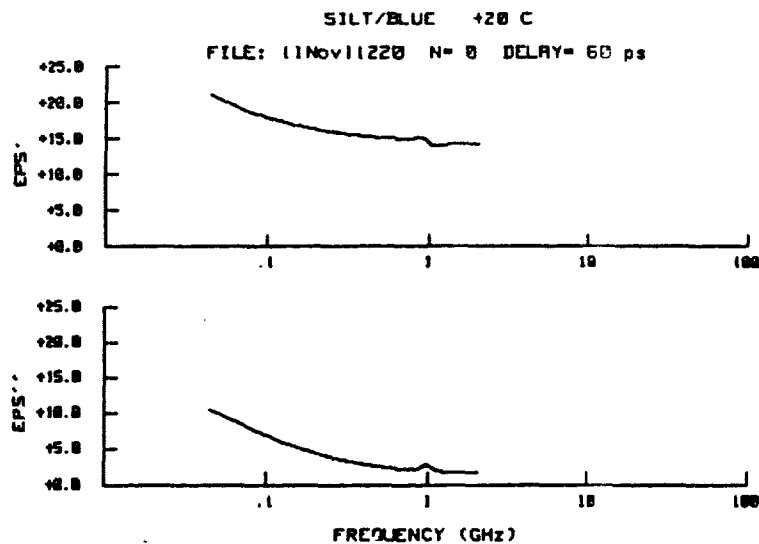
```
482    !  IF Ans$="N" THEN GOTO 473
483    !  COPY Namef$ TO Namef$&":,703"
484    PRINT "STOP (1), RETRIEVE ANOTHER FILE (2), SELECT ANOTHER DELAY (3)"
485    PRINT "MAKE ANOTHER MEASUREMENT (4)"
486    INPUT Seli
487    IF Seli=1 THEN STOP
488    IF Seli=2 THEN GOTO 222
489    IF Seli=3 THEN GOTO 317
490    OUTPUT @Nwa;"ENTO;"
491    OUTPUT @Nwa;"WAIT;CHAN2;S21;CHAN1;S11;"
492    Fd$=DATE$(TIMEDATE)
493    Ft$=TIME$(TIMEDATE)
494    GOTO 263
495    END
```

SILT/BLUE   +20 C

FILE: 11Nov11220   N= 0   DELAY= 60 ps

FREQUENCY (GHz)

START   0.045000000 GHz
STOP   2.045000000 GHz

11 NOV 91
12:22:51

REPORT DOCUMENTATION PAGE		Form Approved OMB No 0704-0188

Public reporting burden for this collection of information is estimated to average 1 hour per response, including the time for reviewing instructions, searching existing data sources, gathering and maintaining the data needed, and completing and reviewing the collection of information. Send comments regarding this burden estimate or any other aspect of this collection of information, including suggestions for reducing this burden, to Washington Headquarters Services, Directorate for Information Operations and Reports, 1215 Jefferson Davis Highway, Suite 1204, Arlington, VA 22202-4302, and to the Office of Management and Budget, Paperwork Reduction Project (0704-0188), Washington, DC 20503

1. AGENCY USE ONLY (Leave blank)	2. REPORT DATE December 1993	3. REPORT TYPE AND DATES COVERED Report 2 of a series

4. TITLE AND SUBTITLE
Microwave Dielectric Behavior of Soils; Report 2,
A Unique Coaxial Measurement Apparatus

5. FUNDING NUMBERS

6. AUTHOR(S)
John O. Curtis

7. PERFORMING ORGANIZATION NAME(S) AND ADDRESS(ES)

U.S. Army Engineer Waterways Experiment Station
Environmental Laboratory
3909 Halls Ferry Road, Vicksburg, MS 39180-6199

8. PERFORMING ORGANIZATION REPORT NUMBER
Technical Report
EL-93-25

9. SPONSORING/MONITORING AGENCY NAME(S) AND ADDRESS(ES)

U.S. Army Corps of Engineers, Washington, DC 20314-1000

10. SPONSORING/MONITORING AGENCY REPORT NUMBER

11. SUPPLEMENTARY NOTES
Available from National Technical Information Service, 5285 Port Royal Road, Springfield, VA 22161.

12a. DISTRIBUTION/AVAILABILITY STATEMENT

Approved for public release; distribution is unlimited.

12b. DISTRIBUTION CODE

13. ABSTRACT (Maximum 200 words)

A reflection/transmission laboratory apparatus and data collection methodology are described that can be used to measure the complex dielectric response of moist soils over the 100 MHz-18 GHz frequency range. The experimental setup includes a square cross-sectional coaxial sample holder, a vector network analyzer system for signal generation and detection, and an external bath for sample temperature control. Data collected on liquids whose dielectric response is well known verify that the electrical property calculation algorithm functions properly.

14. SUBJECT TERMS

Complex dielectric constant	Permittivity
Conductivity	Soil
Microwave	

15. NUMBER OF PAGES
46

16. PRICE CODE

17. SECURITY CLASSIFICATION OF REPORT	18. SECURITY CLASSIFICATION OF THIS PAGE	19. SECURITY CLASSIFICATION OF ABSTRACT	20. LIMITATION OF ABSTRACT
UNCLASSIFIED	UNCLASSIFIED		